Research Square

Preprints are preliminary reports that have not undergone peer review.
They should not be considered conclusive, used to inform clinical practice,
or referenced by the media as validated information.

Unravelling the Antioxidant and ACE-Inhibitory Potential of Lentil Protein Hydrolysates through UHPLC-QTOF-IMS, Tandem Mass Spectrometry and Molecular Docking

Ajay Kumar
Guru Nanak Dev University
Narpinder Singh
narpinders@yahoo.com

Graphic Era (Deemed to be University)
Robin Joshi
University of Pennsylvania

Research Article

Keywords: lentil protein, ACE-inhibitory peptides, antioxidant peptides, UHPLC-QTOF-IMS, MALDI-TOF/TOF, molecular docking, functional food

Posted Date: November 25th, 2026

DOI: https://doi.org/10.21203/rs.3.rs-11572441/v1

License: This work is licensed under a Creative Commons Attribution 4.0 International License.
Read Full License

Additional Declarations:
No competing interests reported.

Table 1 to 4 are available in the Supplementary Files section.

Unravelling the Antioxidant and ACE-Inhibitory Potential of Lentil Protein Hydrolysates through UHPLC-QTOF-IMS, Tandem Mass Spectrometry and Molecular Docking

Ajay Kumar[a], Narpinder Singh[b,*], Robin Joshi[c]

[a] Department of Food Science and Technology, Guru Nanak Dev University, Amritsar, Punjab, India

[b] Department of Food Science and Technology, Graphic Era (Deemed to be University), Dehradun, Uttarakhand, India

[c] Department of Systems Pharmacology and Translational Therapeutics, Institute for Translational Medicine and Therapeutics, University of Pennsylvania, Philadelphia, USA

* Corresponding author. E-mail: narpinders@yahoo.com

Highlights

- Alcalase, trypsin and pepsin generated bioactive lentil protein hydrolysates.
- UHPLC-QTOF-IMS tentatively annotated 174 metabolites across five chemical classes.
- Sequential fractionation enhanced ACE-inhibitory and radical-scavenging activities.
- MALDI-TOF/TOF MS/MS identified three candidate bioactive peptides.
- Molecular docking predicted peptide interactions with human ACE.

Abstract

Lentil (*Lens culinaris*) protein represents an underexplored source of peptides with potential antioxidant and angiotensin-converting enzyme (ACE)-inhibitory activities. This study investigated the effects of alcalase, trypsin and pepsin hydrolysis on lentil protein isolate, integrating non-targeted ultra-high-performance liquid chromatography–quadrupole time-of-flight ion mobility mass spectrometry (UHPLC-QTOF-IMS), sequential peptide fractionation, MALDI-TOF/TOF tandem mass spectrometry (MS/MS) and molecular docking. Alcalase produced the highest degree of hydrolysis (14.83%), followed by trypsin (11.29%) and pepsin (9.47%). Sequential ultrafiltration, Sephadex G-25 gel filtration and reversed-phase high-performance liquid chromatography (RP-HPLC) identified F3B as the most active fraction across the three hydrolysates. The Alcalase-derived F3B fraction exhibited the strongest ACE inhibition, with an IC_{50} of 4.67 ± 0.63 μg/mL, alongside DPPH and ABTS radical-scavenging IC_{50} values of 0.15 ± 0.01 and 1.98 ± 0.08 mg/mL, respectively. The pepsin-derived F3B fraction showed the highest reducing power among the purified fractions. Non-targeted UHPLC-QTOF-IMS profiling tentatively annotated 174 metabolites across the hydrolysates, including amino acid derivatives, lipids, vitamin E-related compounds and other potentially bioactive constituents. MALDI-TOF/TOF MS/MS identified three peptides: RLPALISRHQRL from the Alcalase hydrolysate, RQPAAGEDSSEDLEDNTELLSLVLRA from the trypsin hydrolysate and RLPAGVFFLGNFIGKGD from the pepsin hydrolysate. Molecular docking predicted favourable interactions with human ACE, with the trypsin-derived peptide exhibiting the most negative docking score (−241.4), followed by the pepsin-derived (−222.8) and Alcalase-derived (−180.6) peptides. The difference between docking rankings and experimentally measured inhibition highlights the importance of biochemical validation.

Overall, the findings establish a combined metabolomic and peptidomic workflow for characterizing lentil protein hydrolysates and identify promising candidates for further investigation as antioxidant and ACE-inhibitory food ingredients. Synthetic-peptide validation, gastrointestinal stability assessment and in vivo studies are required to establish their physiological relevance.

Keywords: lentil protein; ACE-inhibitory peptides; antioxidant peptides; UHPLC-QTOF-IMS; MALDI-TOF/TOF; molecular docking; functional food

1. Introduction

Hypertension is a major modifiable risk factor for cardiovascular disease, and angiotensin-converting enzyme (ACE) is a central target for its control because it converts angiotensin I to the vasoconstrictor angiotensin II and inactivates bradykinin. Food-derived peptides that inhibit ACE, and that also scavenge free radicals, have attracted interest as natural alternatives or complements to synthetic inhibitors (Korhonen & Pihlanto, 2006). Such peptides are usually released from food proteins by enzymatic hydrolysis, and their activity depends on chain length, amino acid composition and sequence, with short peptides rich in hydrophobic, aromatic and proline residues generally favoured by the ACE active site (Gómez-Ruiz et al., 2007; Wang et al., 2020).

Legume and oilseed proteins are inexpensive, abundant substrates for such work, and hydrolysates of rapeseed, soybean, sesame and rice bran proteins have been shown to contain enzyme-inhibitory and antioxidant peptides (Wu & Ding, 2002; Yust et al., 2012; Wang et al., 2017; Wang et al., 2020). Our earlier work on rice bran protein showed that alcalase hydrolysis, followed by multi-step purification and mass spectrometric sequencing, yields peptides with both antioxidant and ACE-inhibitory activity (Kumar et al., 2024). Lentil (*Lens culinaris*) proteins, rich in legumin- and vicilin-type globulins, offer a comparable but less explored substrate, and the effect of different proteases on the peptide and metabolite profile of lentil hydrolysates has not been systematically compared.

The aims of this study were therefore to (i) prepare lentil protein isolate and hydrolyse it with alcalase, trypsin and pepsin; (ii) profile the hydrolysates by non-targeted UHPLC-QTOF-IMS; (iii) purify the most active fractions by ultrafiltration, gel filtration and RP-HPLC while tracking antioxidant and ACE-inhibitory activity; (iv) sequence the active fraction by MALDI-TOF/TOF MS/MS; and (v) assess the binding of the identified peptides to human ACE by molecular docking.

2. Materials and methods

2.1. Materials and reagents

Lentil (*Lens culinaris* Medik., variety PL-8) was procured from Punjab Agricultural University, Ludhiana, India. 2,4,6-Trinitrobenzenesulfonic acid (TNBS), L-leucine, Trolox, 2,2′-azino-bis(3-ethylbenzothiazoline-6-sulfonic acid) (ABTS), o-phthaldialdehyde, sodium tetrahydroborate, sodium dodecyl sulfate, mercaptoethanol, rabbit lung ACE, hippuryl-histidyl-leucine (HHL), pepsin (porcine

gastric mucosa, >2500 U/mg) and trypsin (bovine pancreas, 10,000 BAEE U/mg) were obtained from Sigma-Aldrich India. Alcalase 2.4 L (subtilisin Carlsberg) was donated by Novozymes India. Sephadex G-25 was from Sigma Chemical Co. Bovine serum albumin, Bradford reagent and HPLC-grade ethanol, methanol, hexane, acetonitrile, hydrochloric acid and formic acid were from Merck India. All other reagents were of analytical grade.

2.2. Preparation of lentil protein isolate

Whole seeds were dehulled and ground, and the flour was defatted with n-hexane (1:5, w/v) for 6 h in a Soxhlet apparatus and air-dried. Defatted flour was dispersed in deionised water (1:10, w/v), adjusted to pH 9.0 with 1 N NaOH, stirred for 1 h at room temperature and centrifuged (8000 g, 20 min). The pellet was re-extracted once under the same conditions. The combined supernatants were acidified to pH 4.5 with 1 N HCl to precipitate protein, and the precipitate was recovered by centrifugation (8000 g, 20 min, 4 °C), resuspended in deionised water, neutralised to pH 7.0 and freeze-dried to give LPI. Protein content was determined by the Kjeldahl method (N × 6.25).

2.3. Enzymatic hydrolysis and degree of hydrolysis

LPI was hydrolysed at an enzyme-to-substrate ratio of 1:100 with alcalase (pH 8.0, 60 °C, 3 h; 15 U/mg protein), pepsin (pH 2.0, 37 °C, 6 h; 2.5 U/mg protein) or trypsin (pH 8.5, 37 °C, 3 h; 15 U/mg protein). Reactions were stopped by heating at 90 °C for 10 min; after cooling, the mixtures were centrifuged (6000 g, 20 min) and the supernatants were lyophilised and stored at -4 °C. The hydrolysates are designated LBPH-AL, LBPH-PEP and LBPH-TRY. The degree of hydrolysis (DH) was determined by the TNBS method with L-leucine as standard (Rutherfurd, 2010) and expressed as the ratio of free amino groups released to the total amino groups in the intact protein.

2.4. Amino acid analysis

Amino acids were determined by HPLC following AOAC methodology. Samples were hydrolysed with 6 N HCl at 110 °C for 22 h, derivatised with AccQ-Fluor reagent and separated on a Hypersil GOLD C18 column (4.6 × 150 mm, 3 µm) at 1.0 mL/min with a gradient of sodium acetate buffer (pH 4.90) and 60% acetonitrile, using fluorescence detection (excitation 250 nm, emission 395 nm). Quantification used a 17-amino-acid standard mixture; cysteine and methionine were determined after performic acid oxidation and tryptophan after alkaline hydrolysis (4 M NaOH, 105 °C, 24 h). Results are expressed as g/100 g protein.

2.5. Non-targeted UHPLC-QTOF-IMS profiling

Hydrolysates were analysed on an Agilent 6560 ion mobility Q-TOF LC/MS system in positive ionisation mode. Mobile phases were 0.1% formic acid in water (A) and acetonitrile (B), and separation used an Acquity BEH C18 column at 0.3 mL/min. Data were processed with Agilent Mass Profiler Professional, and features differing significantly ($p \leq 0.05$) were annotated against the METLIN and HMDB databases. A heat map was produced in MetaboAnalyst 5.0 (Pareto scaling, hierarchical

clustering), and annotated metabolites were grouped as amino acid derivatives, sugars, lipids, and vitamins and terpenoids.

2.6. Fractionation of the hydrolysates

LBPH (3%, w/v) was fractionated by sequential ultrafiltration through 5 and 3 kDa membranes (CleanNsep Membrane Filtration Equipment Co. Ltd.) into fractions A (<3 kDa), B (3–5 kDa) and C (>5 kDa), which were lyophilised and stored at 4 °C. Fraction A, the most active, was applied (10 mL, 52.57 mg/mL) to a Sephadex G-25 column (2.5 × 60 cm) and eluted with distilled water at 0.2 mL/min (Zhang et al., 2012). Five sub-fractions (F1–F5) were pooled from the elution profile. The most active sub-fraction (F3) was further purified on a Zorbax ODS C18 column (4.6 × 250 mm, 5 μm; Agilent) with an acetonitrile gradient of 5–25% (v/v) over 0–30 min, held at 25% from 30 to 50 min, at 1.0 mL/min with detection at 215 and 280 nm. Four peaks (F3A–F3D) were collected and lyophilised.

2.7. Antioxidant assays

DPPH radical scavenging was measured as described by Marinova and Batchvarov (2011): 500 μL of sample was mixed with 500 μL of 0.02% DPPH in ethanol, incubated for 30 min in the dark, and absorbance read at 517 nm; glutathione served as positive control. ABTS radical scavenging followed Kumar et al. (2024): $ABTS^{\bullet+}$ was generated with potassium persulfate, diluted to A_{734} 0.70 ± 0.05, mixed with sample (20 μL + 980 μL) and read after 10 min at 734 nm. Reducing power was determined by the potassium ferricyanide method of Liu et al. (2009), with ascorbic acid and (+)-catechin as references and absorbance read at 700 nm. Scavenging activity (%) was calculated as $[(A_{control} - A_{sample})/A_{control}] \times 100$, and IC_{50} values were obtained by non-linear regression of dose–response curves.

2.8. ACE-inhibitory activity

ACE inhibition was measured by the method of Cushman and Cheung (1971) with minor modifications. Sample (30 μL), 5 mmol/L HHL (80 μL) and 0.1 M borate buffer, pH 8.3 (30 μL) were pre-incubated at 37 °C for 5 min, then ACE (10 μL, 0.1×10^3 U/L) was added and incubated for 30 min at 37 °C. The reaction was stopped with 1 mol/L HCl (150 μL), and hippuric acid was quantified by RP-HPLC on a Kromasil 100-5C18 column (250 × 4.6 mm, 5 μm) with isocratic 15% methanol at 0.4 mL/min and detection at 228 nm. Inhibition (%) = $[(A_1 - A_2)/A_1] \times 100$, where A_1 and A_2 are hippuric acid peak areas without and with sample.

2.9. Peptide sequencing by MALDI-TOF/TOF MS/MS

Purified fractions were co-crystallised with α-cyano-4-hydroxycinnamic acid (0.1% trifluoroacetic acid, 30% acetonitrile; 1:2 sample:matrix) on an Anchor Chip target and analysed on a Bruker UltrafleXtreme in positive reflector mode over 700–4000 Da (500 laser shots per spectrum). Precursors were fragmented by LIFT technology, the instrument was calibrated with a tryptic BSA digest, and sequences were derived by de novo interpretation in BioTools 3.0. The peptides reported here originated

from the following spectra: LPI trypsin (spectrum 2602), LPI pepsin (spectrum 1651) and LPI alcalase (spectrum 1190).

2.10. Peptide properties and molecular docking

Theoretical monoisotopic masses, net charge at pH 7.0, isoelectric point and grand average of hydropathy (GRAVY; Kyte–Doolittle scale) were calculated from the sequences. Three-dimensional peptide structures were predicted with PEP-FOLD3 (Lamiable et al., 2016). The crystal structure of human ACE (PDB: 1O8A) was prepared by removing lisinopril and water while retaining the zinc and chloride ions, and the peptides were docked to the enzyme with a flexible peptide–protein docking server (Kurcinski et al., 2015)]. Complexes were inspected in PyMOL 2.5. Docking scores are dimensionless, with more negative values indicating more favourable predicted binding.

2.11. Statistical analysis

All measurements were made in triplicate and are reported as mean ± SD. Differences were tested by one-way ANOVA followed by Duncan's multiple range test ($p \leq 0.05$) in Minitab 19.

3. Results and discussion

3.1. Degree of hydrolysis

At equal protein concentration, alcalase gave the highest DH (14.83 ± 0.41%), followed by trypsin (11.29 ± 0.34%) and pepsin (9.47 ± 0.28%) (Table 1). The higher DH with alcalase reflects its broad specificity as a serine endoproteinase that cleaves preferentially next to large uncharged residues, and its high activity at alkaline pH. Trypsin is restricted to arginine and lysine bonds, which are abundant in lentil legumin and vicilin, and so gave an intermediate DH. The lowest DH with pepsin may reflect the compact, acid-stable structure of the storage proteins and limited access to cleavage sites at pH 2.0. The same ranking was reported for rice bran protein (Kumar et al., 2024), where alcalase gave a DH of 12.61%. A higher DH is generally associated with greater hydrophilicity and net charge of the peptide pool, which favours absorption and may reduce allergenicity (Liu et al., 2018).

3.2. Amino acid composition

LPI had a total amino acid content of 96.72 g/100 g protein, dominated by glutamic acid (17.64 g/100 g) and aspartic acid (11.43 g/100 g), the typical acidic profile of legume globulins (Table 2). Lysine (7.83 g/100 g), leucine (7.21 g/100 g) and arginine (6.94 g/100 g) were also abundant, supporting the nutritional quality of the protein. Hydrolysis changed the free amino acid pool markedly. LBPH-AL had the highest levels of essential amino acids, including methionine (0.258 g/100 g), lysine (0.238 g/100 g) and leucine (0.247 g/100 g), and was enriched in amino acids associated with radical scavenging by electron or hydrogen donation (tyrosine, histidine, tryptophan, proline, alanine, leucine). Hydrophobic residues (Val, Ile, Leu, Phe, Pro) exceeded 38% of the amino acids in all hydrolysates, which favours hydrophobic contacts with the S1 and S2 pockets of ACE (Gómez-Ruiz et al., 2007).

Branched-chain amino acids were especially enriched in LBPH-AL, consistent with the preference of alcalase for non-polar P1 residues.

3.3. Non-targeted metabolite profile of the hydrolysates

UHPLC-QTOF-IMS profiling of LBPH-AL, LBPH-TRY and LBPH-PEP tentatively annotated 174 metabolites belonging to five major classes: amino acids and derivatives (n = 68), sugars and derivatives (n = 20), lipids and derivatives (n = 30), vitamins and terpenoids (n = 26), and flavonoids, phenolics and their derivatives (n = 30) (Fig. 1). The metabolites were tentatively assigned based on accurate mass, retention time, ion-mobility characteristics and available MS/MS spectral/database information. Similar non-targeted UHPLC-QTOF-IMS approaches have previously demonstrated the ability to characterize a broad range of metabolites and potential bioactive compounds in plant protein hydrolysates (Kumar et al., 2024).

Among the amino acid derivatives, pyroglutamic acid, isoleucyl-valine, N-acetyltryptophan and hydroxyprolyl-lysine were more abundant in LBPH-AL and LBPH-TRY than in LBPH-PEP. Agmatine and citrulline were detected in all three hydrolysates. Citrulline is metabolically linked to arginine availability and nitric oxide (NO) synthesis, whereas agmatine is an endogenous decarboxylated derivative of arginine that can modulate nitric oxide synthase and vascular signalling (Raghavan & Dikshit, 2004; Molderings & Haenisch, 2012). Agmatine has also been reported to stimulate NO production in endothelial cells under experimental conditions (Galea et al., 1996). Therefore, the presence of these metabolites may indicate the occurrence of compounds associated with arginine/NO metabolism; however, their detection in the hydrolysates alone does not establish a physiological vasodilatory effect.

Several vitamin E-related metabolites, including α-tocopherol, γ-tocopherol, γ-tocotrienol and δ-tocotrienol, were detected in all three hydrolysates. α-Tocopherol has been reported to inhibit protein kinase C activity and vascular smooth muscle cell proliferation at physiologically relevant concentrations (Tasinato et al., 1995). These effects are considered to involve signalling mechanisms in addition to the classical antioxidant activity of vitamin E. Previous metabolomic profiling of rice bran protein hydrolysates also identified tocopherols and tocotrienols together with other potentially bioactive metabolites, demonstrating the relevance of non-targeted UHPLC-QTOF-IMS for characterizing co-extracted micronutrient and lipid-derived compounds in protein hydrolysates (Kumar et al., 2024). However, the biological activity of the vitamin E compounds detected in the present study should not be inferred directly from their qualitative or relative abundance.

Taurine was particularly prominent in the Alcalase hydrolysate, whereas pyridoxine (vitamin B6) was detected in all three hydrolysates. The detection of these compounds further demonstrates that enzymatic hydrolysis and downstream fractionation can retain low-molecular-weight nitrogenous and micronutrient-associated compounds in addition to peptides. N-Acetyltryptophan, which was more

abundant in LBPH-AL, has been used as a stabilizing ligand in protein formulations and has been reported to reduce oxidative modification of human serum albumin under certain experimental conditions (Fang et al., 2011; Anraku et al., 2004). Thus, its detection in LBPH-AL may be of interest from a functional perspective, although its biological relevance within lentil hydrolysates requires further targeted investigation.

Among the sugar-related metabolites, β-D-glucopyranosyl glucoside and methyl isomaltoside were relatively enriched in LBPH-PEP, whereas **2**8-glucosylsiaresinolate 3-arabinoside showed the highest abundance in LBPH-AL. The latter compound is chemically a glycosylated triterpenoid, and its classification within the broad sugar/derivative group should therefore be interpreted as a metabolomic grouping rather than a strict structural classification. Such glycosylated secondary metabolites can occur naturally in legume matrices and may be released or differentially extracted during protein isolation and enzymatic hydrolysis.

Several lipid-related metabolites, including LysoPE(0:0/20:1), PG(18:0/22:5) and 6-(α-D-glucosaminyl)-1D-myo-inositol, were relatively more abundant in the Alcalase fraction. 16-Hydroxyhexadecanoic acid was detected in all three hydrolysates, indicating the persistence of long-chain hydroxy fatty-acid derivatives following hydrolysis. Similar lipid-derived compounds, including lysophospholipids and hydroxy fatty acids, have been reported during non-targeted metabolomic characterization of plant protein hydrolysates (Kumar et al., 2024).

Overall, LBPH-AL exhibited the richest profile of potentially bioactive co-extracted metabolites, including amino acid derivatives, vitamin E-related compounds, phospholipids, fatty-acid derivatives and secondary metabolites. These compounds may contribute to the overall antioxidant and ACE-inhibitory characteristics of the crude hydrolysate in addition to the peptides identified by peptide sequencing and molecular docking. Nevertheless, this interpretation should be considered hypothesis-generating, because metabolite annotation and relative abundance do not establish biological activity. Targeted quantitative analysis and individual metabolite bioassays would be required to determine their contribution to the observed activities. To our knowledge, the present study provides a detailed non-targeted UHPLC-QTOF-IMS characterization of the metabolite composition of lentil protein hydrolysates generated using Alcalase, trypsin and pepsin.

[Figure 1 to be inserted] **3.4. Antioxidant activity through the purification cascade**

Lower IC_{50} values denote stronger activity. The three crude hydrolysates had similar DPPH IC_{50} values (1.52–1.63 mg/mL) and ABTS IC50 values (23.85–25.42 mg/mL) (Table 3a), indicating that enzyme choice alone had a modest effect on radical scavenging. Fractionation had a much larger effect. Ultrafiltration fraction A (<3 kDa) was significantly more active than the 3–5 kDa and >5 kDa fractions for all enzymes, in agreement with the higher activity of low-molecular-weight peptides reported for rice bran hydrolysates (Wang et al., 2017). Sephadex G-25 sub-fraction F3 lowered the DPPH IC50 to

0.26, 0.29 and 0.34 mg/mL (AL, TRY, PEP), and RP-HPLC peak F3B reached 0.15 ± 0.01, 0.17 ± 0.02 and 0.21 ± 0.01 mg/mL, a 7- to 11-fold gain over the crude hydrolysates. ABTS IC50 fell from 23.85–25.42 mg/mL to 1.98 ± 0.08 (AL), 3.11 ± 0.12 (TRY) and 2.07 ± 0.08 mg/mL (PEP), an 8- to 13-fold gain. Small peptides expose Tyr, His, Trp and Cys residues more readily for electron or hydrogen donation to radicals, and their lower mass improves access to hydrophobic radical species.

3.5. Reducing power

The reducing power of LBPH (crude hydrolysate) and its purified fractions was evaluated by measuring absorbance at 700 nm (A700), with higher absorbance indicating greater reducing capacity (Oyaizu, 1986). As shown in Table 3b, the reducing power varied with both the proteolytic enzyme and purification stage. The crude hydrolysates exhibited A700 values of 0.187 ± 0.007, 0.204 ± 0.004, and 0.269 ± 0.005 for Alcalase-, trypsin-, and pepsin-derived samples, respectively. Following ultrafiltration, the reducing power decreased to 0.091 ± 0.003, 0.109 ± 0.003, and 0.138 ± 0.003, respectively. However, Sephadex fractionation increased the corresponding values to 0.161 ± 0.006, 0.172 ± 0.005, and 0.182 ± 0.004, suggesting enrichment or selective recovery of components with electron-donating capacity. The RP-HPLC-purified F3B fractions exhibited values of 0.072 ± 0.003, 0.079 ± 0.002, and 0.089 ± 0.002 for Alcalase, trypsin, and pepsin, respectively. Although these values were lower than those of the crude hydrolysates and Sephadex fractions, the purified pepsin-derived fraction retained the highest reducing power among the three F3B samples. These findings suggest that antioxidant reducing capacity depends on the enzyme used for hydrolysis and the composition of the resulting peptide fractions. Food-derived peptides can contribute to antioxidant activity through electron donation and other mechanisms, although reducing power alone does not establish their overall antioxidant efficacy (Zhu et al., 2022; Chalamaiah et al., 2022). The lower A700 values after RP-HPLC purification may reflect the removal of other reducing components or the isolation of a narrower peptide population, rather than necessarily indicating a loss of biological value.

3.6 ACE-inhibitory activity

ACE inhibition showed the clearest enzyme effect. Crude LBPH-AL was the most potent (IC50 128.74 ± 18.43 µg/mL), ahead of LBPH-TRY (256.38 ± 24.71 µg/mL) and LBPH-PEP (319.84 ± 21.69 µg/mL). The <3 kDa fraction of LBPH-AL had an IC_{50} of 68.24 ± 9.83 µg/mL, consistent with better access of small peptides to the narrow, zinc-containing active site. Sub-fraction F3 gave IC50 values of 13.27 ± 1.87, 21.39 ± 2.03 and 28.76 ± 1.97 µg/mL (AL, TRY, PEP), and RP-HPLC fraction F3B reached 4.67 ± 0.63, 9.14 ± 0.87 and 17.23 ± 1.19 µg/mL, a 19- to 28-fold improvement over the crude hydrolysates. The F3B value for alcalase compares favourably with the soybean peptide fraction described by Wu and Ding (2002; IC50 8.2 µg/mL), although fraction-level values should not be equated with those of single purified peptides. The superior performance of alcalase fractions agrees

with Kumar et al. (2024), who linked it to the enzyme's release of hydrophobic residues at peptide C-termini, which ACE prefers.

3.6. Identification of peptides in fraction F3B through MALDI-TOF/TOF MS/MS

MALDI-TOF/TOF MS/MS sequencing of fraction F3B resulted in the identification of one peptide from each enzymatic hydrolysate (Table 4): RLPALISRHQRL (12 residues) from the Alcalase hydrolysate**,** RQPAAGEDSSEDLEDNTELLSLVLRA (26 residues) from the trypsin hydrolysate, RLPAGVFFLGNFIGKGD (17 residues) from the pepsin hydrolysate. The calculated molecular masses of the identified peptides were consistent with their recovery in the <3 kDa fraction. Although the trypsin-derived peptide contains 26 residues, its calculated molecular mass (2.83 kDa) remained below the ultrafiltration cut-off. The molecular size, amino acid composition, hydrophobicity and terminal residues are important determinants of ACE-inhibitory peptide activity (Korhonen & Pihlanto, 2006; Lu et al., 2023).

The molecular masses of the three peptides identified in fraction F3B were evaluated by comparing the experimentally observed MALDI-TOF/TOF precursor-ion signals with the theoretical masses calculated from their amino acid sequences. The observed mass values were 1190, 2602 and 1651 Da (Figure 2a,2b,& 2c)for the Alcalase-derived peptide RLPALISRHQRL, trypsin-derived peptide RQPAAGEDSSEDLEDNTELLSLVLRA and pepsin-derived peptide RLPAGVFFLGNFIGKGD, respectively. Peptide identification by mass spectrometry relies on precursor-ion mass measurements together with characteristic fragment-ion patterns generated during tandem MS/MS analysis (Egelhofer et al., 2002). The accuracy of the measured peptide masses also depends on instrument calibration and the mass range of the analyte, as demonstrated by Gobom et al. (2002). Consequently, the observed mass values should be interpreted alongside the fragmentation data rather than being used as the sole criterion for assigning peptide sequences.

Comparison of the observed and theoretical values indicated differences that should be verified before finalizing Table 4. The calculated ($[M+H]^+$) values were 1195.390, 2605.88 and 1651.35 Da or the Alcalase-, trypsin- and pepsin-derived peptides, respectively. The corresponding reported observed values differed by approximately 5.39, 3.88 and 0.35 Da. Because monoisotopic mass, average molecular mass and measured precursor-ion (m/z) are distinct quantities, these values should not be compared until the mass convention and ion assignment have been confirmed. Calibration errors can affect mass accuracy, and appropriate calibration is important for reliable peptide mass determination (Gobom et al., 2002)

The three peptides displayed markedly different physicochemical characteristics. RLPALISRHQRL, identified from the Alcalase hydrolysate, showed the highest predicted positive charge (+3.0), a basic pI of 12.8 and a relatively moderate hydrophobicity (GRAVY −0.41). Its sequence contains several

positively charged residues, particularly Arg and His, together with Leu and Ile residues. Positively charged and hydrophobic residues, especially those positioned toward the C-terminal region, have frequently been associated with ACE-inhibitory activity because they can promote electrostatic and hydrophobic interactions within the ACE substrate-binding subsites (Wu et al., 2006; Lu et al., 2019). However, the C-terminal Leu of RLPALISRHQRL differs from the commonly reported preference for aromatic residues or Pro at the C-terminus of many potent ACE-inhibitory peptides, indicating that its predicted activity may arise from a combination of interactions rather than a single terminal-residue feature.

The pepsin-derived peptide, RLPAGVFFLGNFIGKGD, exhibited a positive GRAVY value (+0.46), indicating comparatively high hydrophobicity, with approximately 53% hydrophobic residues. The presence of Phe-Phe and other hydrophobic residues may favour insertion into hydrophobic regions of the ACE binding cavity. Hydrophobic and aromatic residues have been frequently implicated in ACE recognition and inhibitory activity, particularly around the C-terminal region of peptide inhibitors (Wu et al., 2006; Lu et al., 2023). Nevertheless, the C-terminal Asp residue of this peptide is less characteristic of classical potent ACE-inhibitory sequences, and therefore its docking behaviour provides useful additional information regarding its possible binding mode.

In contrast, the trypsin-derived peptide RQPAAGEDSSEDLEDNTELLSLVLRA was strongly acidic, with a predicted net charge of −5.1 and pI of 3.7. Its relatively low GRAVY value (−0.65) indicates a predominantly hydrophilic character resulting from multiple Asp and Glu residues. Thus, its potential interaction with ACE is expected to differ from that of the more hydrophobic and positively charged peptides. The presence of Leu-rich regions toward the C-terminal portion may nevertheless permit hydrophobic contacts within the ACE binding cavity. These differences highlight the importance of considering the overall sequence and three-dimensional interaction pattern rather than predicting ACE inhibition solely from peptide charge or hydrophobicity.

Interestingly, the two peptides RLPAGVFFLGNFIGKGD and RLPALISRHQRL share the N-terminal motif RLPA, suggesting that they may originate from related regions of lentil storage proteins. This observation should preferably be confirmed by an *in silico* search against the *Lens culinaris* proteome before assigning a specific precursor protein. The presence of Pro at the second or third position may also contribute to resistance against some proteolytic enzymes, although gastrointestinal stability cannot be concluded solely from sequence composition (Lu et al., 2019).

3.7 Molecular docking with ACE

Molecular docking was subsequently performed against the crystal structure of human ACE (PDB ID: 1O8A), which provides an experimentally determined structural model of the human ACE catalytic domain (Natesh et al., 2003). The docking results showed negative predicted binding scores for all three peptides, with values of −241.4, −222.8 and −180.6 for the trypsin-, pepsin- and Alcalase-derived

peptides, respectively (Table 4). Within the scoring framework used in the present study, the increasingly negative value indicates a more favourable predicted peptide–ACE interaction. Accordingly, the trypsin-derived peptide exhibited the most favourable docking score, followed by the pepsin- and Alcalase-derived peptides. These docking scores should, however, be interpreted as comparative computational predictions rather than direct measures of ACE-inhibitory potency.

The three-dimensional docking image for RLPALISRHQRL–ACE (Fig. 3a) illustrates the peptide positioned within a surface-accessible cleft of the ACE structure. The ACE protein is represented as a ribbon structure, whereas the docked peptide is shown as a stick representation near the binding region. The labelled residues indicate the principal residue-level contacts predicted by the docking calculation. In particular, interactions involving Arg and Glu/Asp residues of ACE suggest that electrostatic interactions may contribute to stabilization of the positively charged RLPALISRHQRL peptide. The multiple Arg residues within the peptide provide positively charged guanidinium groups capable of forming favourable electrostatic and hydrogen-bonding interactions with negatively charged residues in the ACE binding environment. Such interactions are consistent with the established importance of peptide charge and amino acid composition in ACE recognition (Lu et al., 2019; Lu et al., 2023).

Molecular docking was performed to investigate the binding interaction of the Alcalase-derived lentil peptide RLPALISRHQRL with human angiotensin-converting enzyme (ACE; PDB ID: 1O8A). The peptide exhibited a docking score of −180.6, indicating a favourable predicted interaction within the scoring framework used in this study. As illustrated in Figure 6, the peptide (cyan stick/ribbon representation) is positioned near a surface-accessible region of the ACE structure (red ribbon representation), with the docked pose suggesting potential interactions between the peptide and residues lining the binding region. The peptide contains three arginine residues, one histidine and several hydrophobic residues, including leucine and isoleucine, which may contribute to electrostatic, hydrogen-bonding and hydrophobic interactions, respectively. These sequence features provide a plausible basis for peptide–protein recognition; however, the specific interaction types and participating amino acid residues should be confirmed using residue-level interaction analysis and interatomic distances. Overall, the docking result supports further investigation of RLPALISRHQRL as a potential ACE-inhibitory peptide.

Molecular docking was used to investigate the predicted interaction of the trypsin-derived lentil protein hydrolysate peptide with human angiotensin-converting enzyme (ACE; PDB ID: 1O8A). As shown in the figure, the peptide is positioned along a surface region of ACE, with the labeled residues Asn337–Glu11, Arg313–Glu11, Lys317–Asp15, and Arg25–Leu430 indicating the contacts reported in the docking visualization. These contacts suggest that the predicted peptide–ACE association may involve a combination of polar or electrostatic interactions and local structural complementarity. Such interactions are relevant to ACE–peptide recognition, as previous studies have shown that peptide sequence and residue-specific interactions can influence ACE binding and inhibition (Wu et al., 2006;

Anthony et al., 2012). However, the figure alone does not establish the precise interaction type or demonstrate inhibition of enzyme activity.

Molecular docking analysis revealed a predicted interaction between the pepsin-derived peptide and angiotensin-converting enzyme (ACE), as illustrated in Figure X. The docked complex shows the peptide positioned in proximity to the ACE protein structure, with the annotated residue contacts suggesting potential contributions from local electrostatic interactions and hydrogen bonding, depending on the interaction geometry. The observed contacts, including the annotated residue pairs Gln231–Leu9, Glu234–Asp17, and Asp473–Arg1, may contribute to the stabilization of the peptide–ACE complex. Such interactions are relevant because food-derived peptides can potentially inhibit ACE by occupying regions involved in substrate recognition or by interacting with residues associated with its catalytic centre. Previous molecular docking studies have demonstrated that peptide–ACE binding can involve hydrogen bonds, hydrophobic interactions, and contacts with residues surrounding the catalytic zinc-binding site (Chamata et al., 2020; Li et al., 2023).

Figure 3(a) also shows that the peptide is located close to the ACE substrate-binding region rather than being positioned randomly on the protein surface. The predicted contacts labelled in the structure, including interactions involving ARG8, ARG1, GLU441 and LEU12, indicate that both electrostatic and hydrophobic contributions may participate in complex stabilization. The Arg residues of RLPALISRHQRL can provide favourable charge-assisted interactions, while Leu residues can participate in hydrophobic contacts with non-polar regions of the ACE binding pocket. The combination of these interactions may explain why the Alcalase-derived peptide produced a favourable docking score despite its relatively low overall GRAVY value.

The docking results for the three peptides further demonstrate that sequence-dependent interaction patterns can differ substantially among peptides generated by different proteases. The trypsin-derived peptide produced the most negative docking score (−241.4), despite being strongly acidic, suggesting that its favourable predicted binding may result from a combination of multiple hydrogen-bond/electrostatic contacts and interactions involving its Leu-rich C-terminal region. The pepsin-derived peptide showed an intermediate score (−222.8), consistent with its comparatively high hydrophobicity and aromatic Phe residues. The Alcalase-derived peptide displayed a less negative score (−180.6), although its positively charged Arg-rich sequence generated several visible contacts with ACE residues in the docking pose. Thus, the docking analysis indicates that ACE binding is governed by the collective contribution of peptide size, charge, hydrophobicity, aromatic residues and specific residue positioning rather than by any single sequence descriptor (Wu et al., 2006; Lu et al., 2019; Lu et al., 2023).

Importantly, molecular docking provides a mechanistic hypothesis for peptide–ACE recognition but does not establish inhibitory activity experimentally. Therefore, the docking results should be

considered complementary to the ACE-inhibitory assay and MS/MS identification. The peptide showing the most favourable docking score, particularly RQPAAGEDSSEDLEDNTELLSLVLRA, warrants further validation using synthetic peptide and purified ACE inhibition assays, followed by gastrointestinal stability and bioavailability studies.

4. Conclusion

This study demonstrates the potential of lentil (*Lens culinaris*) protein as a source of antioxidant and angiotensin-converting enzyme (ACE)-inhibitory peptides, with the observed bioactivity strongly influenced by the proteolytic enzyme and subsequent purification. Among the enzymes investigated, Alcalase produced the highest degree of hydrolysis (14.83%) and the most potent ACE-inhibitory activity, while sequential ultrafiltration, Sephadex G-25 gel filtration and RP-HPLC substantially enhanced the activity of the resulting peptide fractions. The final F3B fraction obtained from the Alcalase hydrolysate exhibited the strongest ACE inhibition (IC_{50} = 4.67 ± 0.63 μg/mL), accompanied by substantial DPPH and ABTS radical-scavenging activities. Reducing-power measurements further revealed enzyme-dependent differences in electron-donating capacity, with the pepsin-derived F3B fraction exhibiting the highest absorbance among the purified fractions. Non-targeted UHPLC-QTOF-IMS profiling provided a broad overview of the metabolite composition of the hydrolysates, highlighting their chemical complexity beyond peptide constituents. MALDI-TOF/TOF MS/MS identified three peptides derived from the Alcalase, trypsin and pepsin hydrolysates, while molecular docking predicted favourable interactions between these peptides and human ACE. Notably, the trypsin-derived peptide exhibited the most favourable docking score, whereas the Alcalase-derived fraction demonstrated the strongest experimentally measured ACE-inhibitory activity, emphasizing that predicted binding scores do not necessarily correspond directly to inhibitory potency. Collectively, these findings establish an integrated analytical approach for identifying and characterizing potentially bioactive peptides from lentil proteins and support further investigation of their applications in functional food development. Nevertheless, validation using synthetic peptides, purified-enzyme inhibition kinetics, gastrointestinal digestion and stability studies, and appropriate in vivo models is required to establish their mechanisms of action, bioavailability and physiological relevance.

Ethics and consent to participate

The plant material used in this study consisted of lentil (*Lens culinaris* Medik., variety PL-8) seeds procured from Punjab Agricultural University (PAU), Ludhiana, Punjab, India. The study involved the use of procured plant material for laboratory-based protein extraction, enzymatic hydrolysis and biochemical characterization. No wild plants or plant parts were collected directly from natural habitats or protected areas. The plant material was obtained and used in accordance with applicable institutional and national guidelines. As the study involved procured seeds rather than field collection, no separate field collection permit or licence was applicable. No human participants or live animals were involved in this study.

Declaration of competing interest

The authors declare that they have no known competing financial interests or personal relationships that could have appeared to influence the work reported in this paper.

Declaration of Competing Interest

The author declares that there is no known competing financial interest or personal relationship that could have appeared to influence the work reported in this paper.

Funding: The authors declare that no external funding was received for the preparation of this review**.**

Conflict of Interest: The authors declare no conflict of interest.

Data Availability Statement

The datasets generated and/or analysed during the current study are available from the corresponding author upon reasonable request.

CRediT authorship contribution statement

Ajay Kumar: Conceptualization, Formal analysis, Data curation, Writing -original draft. **Narpinder Singh:** Conceptualization, Investigation, Supervision, Formal analysis, Funding acquisition, Writing - review & editing. **Robin Joshi:** Mass spectrometry acquisition and data analysis, Writing - review & editing.

References

Cushman, D. W., & Cheung, H. S. (1971). Spectrophotometric assay and properties of the angiotensin-converting enzyme of rabbit lung. *Biochemical pharmacology*, *20*(7), 1637-1648.

Gómez-Ruiz, J. Á., Ramos, M., & Recio, I. (2007). Identification of novel angiotensin-converting enzyme-inhibitory peptides from ovine milk proteins by CE-MS and chromatographic techniques. *Electrophoresis*, *28*(22), 4202-4211.

Korhonen, H., & Pihlanto, A. (2006). Bioactive peptides: production and functionality. *International dairy journal*, *16*(9), 945-960.

Kumar, A., Singh, N., & Joshi, R. (2024). Evaluation of antioxidant and ACE inhibitory peptides in rice bran protein hydrolysate using non-targeted UHPLC-QTOF-IMS profiling, MALDI-TOF-TOF-MS/MS, and molecular docking study. *International Journal of Food Science and Technology*, *59*(6), 4300-4314.

Kurcinski, M., Jamroz, M., Blaszczyk, M., Kolinski, A., & Kmiecik, S. (2015). CABS-dock web server for the flexible docking of peptides to proteins without prior knowledge of the binding site. *Nucleic acids research*, *43*(W1), W419-W424.

Anraku, M., Tsurusaki, Y., Watanabe, H., Maruyama, T., Kragh-Hansen, U., & Otagiri, M. (2004). Stabilizing mechanisms in commercial albumin preparations: octanoate and N-acetyl-L-tryptophanate protect human serum albumin against heat and oxidative stress. *Biochimica et Biophysica Acta (BBA)-Proteins and Proteomics*, *1702*(1), 9-17.

Fang, L., Parti, R., & Hu, P. (2011). Characterization of N-acetyltryptophan degradation products in concentrated human serum albumin solutions and development of an automated high performance liquid chromatography–mass spectrometry method for their quantitation. *Journal of chromatography A*, *1218*(41), 7316-7324.

Lamiable, A., Thévenet, P., Rey, J., Vavrusa, M., Derreumaux, P., & Tufféry, P. (2016). PEP-FOLD3: faster de novo structure prediction for linear peptides in solution and in complex. *Nucleic acids research*, *44*(W1), W449-W454.

Liu, C., Ma, X., Che, S., Wang, C., & Li, B. (2018). The effect of hydrolysis with neutrase on molecular weight, functional properties, and antioxidant activities of Alaska pollock protein isolate. *Journal of Ocean University of China*, *17*(6), 1423-1431.

Liu, S. C., Lin, J. T., Wang, C. K., Chen, H. Y., & Yang, D. J. (2009). Antioxidant properties of various solvent extracts from lychee (Litchi chinenesis Sonn.) flowers. *Food Chemistry*, *114*(2), 577-581.

Marinova, G., & Batchvarov, V. (2011). Evaluation of the methods for determination of the free radical scavenging activity by DPPH. *Bulgarian Journal of Agricultural Science*, *17*(1), 11-24.

Rutherfurd, S. M. (2010). Methodology for determining degree of hydrolysis of proteins in hydrolysates: a review. *Journal of AOAC International*, *93*(5), 1515-1522.

Wang, R., Lu, X., Sun, Q., Gao, J., Ma, L., & Huang, J. (2020). Novel ACE inhibitory peptides derived from simulated gastrointestinal digestion in vitro of sesame (Sesamum indicum L.) protein and molecular docking study. *International journal of molecular sciences*, *21*(3), 1059.

Wang, X., Chen, H., Fu, X., Li, S., & Wei, J. (2017). A novel antioxidant and ACE inhibitory peptide from rice bran protein: Biochemical characterization and molecular docking study. *Lwt*, *75*, 93-99.

Wu, J., & Ding, X. (2002). Characterization of inhibition and stability of soy-protein-derived angiotensin I-converting enzyme inhibitory peptides. *Food research international*, *35*(4), 367-375.

del Mar Yust, M., Pedroche, J., Megías, C., Girón-Calle, J., Alaiz, M., Millán, F., & Vioque, J. (2004). Rapeseed protein hydrolysates: a source of HIV protease peptide inhibitors. *Food chemistry*, *87*(3), 387-392.

Zhang, Y., Duan, X., & Zhuang, Y. (2012). Purification and characterization of novel antioxidant peptides from enzymatic hydrolysates of tilapia (Oreochromis niloticus) skin gelatin. *Peptides*, *38*(1), 13-21.

Anraku, M., Tsurusaki, Y., Watanabe, H., Maruyama, T., Kragh-Hansen, U., & Otagiri, M. (2004). Stabilizing mechanisms in commercial albumin preparations: octanoate and N-acetyl-L-tryptophanate protect human serum albumin against heat and oxidative stress. *Biochimica et Biophysica Acta (BBA)-Proteins and Proteomics*, *1702*(1), 9-17.

Fang, L., Parti, R., & Hu, P. (2011). Characterization of N-acetyltryptophan degradation products in concentrated human serum albumin solutions and development of an automated high performance liquid chromatography–mass spectrometry method for their quantitation. *Journal of chromatography A*, *1218*(41), 7316-7324.

Kumar, A., Singh, N., & Joshi, R. (2024). Evaluation of antioxidant and ACE inhibitory peptides in rice bran protein hydrolysate using non-targeted UHPLC-QTOF-IMS profiling, MALDI-TOF-TOF-MS/MS, and molecular docking study. *International Journal of Food Science and Technology*, *59*(6), 4300-4314.

Molderings, G. J., & Haenisch, B. (2012). Agmatine (decarboxylated L-arginine): physiological role and therapeutic potential. *Pharmacology & Therapeutics*, *133*(3), 351-365.

Raghavan, S. A., & Dikshit, M. (2004). Vascular regulation by the L-arginine metabolites, nitric oxide and agmatine. *Pharmacological research*, *49*(5), 397-414.

Tasinato, A., Boscoboinik, D., Bartoli, G. M., Maroni, P., & Azzi, A. (1995). d-alpha-tocopherol inhibition of vascular smooth muscle cell proliferation occurs at physiological concentrations, correlates with protein kinase C inhibition, and is independent of its antioxidant properties. *Proceedings of the National Academy of Sciences*, *92*(26), 12190-12194.

Korhonen, H., & Pihlanto, A. (2006). Bioactive peptides: production and functionality. *International dairy journal*, *16*(9), 945-960.

Xue, L., Yin, R., Howell, K., & Zhang, P. (2021). Activity and bioavailability of food protein-derived angiotensin-I-converting enzyme–inhibitory peptides. *Comprehensive Reviews in Food Science and Food Safety*, *20*(2), 1150-1187.

Xiang, L., Qiu, Z., Zhao, R., Zheng, Z., & Qiao, X. (2023). Advancement and prospects of production, transport, functional activity and structure-activity relationship of food-derived angiotensin converting enzyme (ACE) inhibitory peptides. *Critical reviews in food science and nutrition*, *63*(10), 1437-1463.

Fan, H., Liao, W., & Wu, J. (2019). Molecular interactions, bioavailability, and cellular mechanisms of angiotensin-converting enzyme inhibitory peptides. *Journal of Food Biochemistry*, *43*(1), e12572.

Natesh, R., Schwager, S. L., Sturrock, E. D., & Acharya, K. R. (2003). Crystal structure of the human angiotensin-converting enzyme–lisinopril complex. *Nature*, *421*(6922), 551-554.

Wu, J., Aluko, R. E., & Nakai, S. (2006). Structural requirements of angiotensin I-converting enzyme inhibitory peptides: Quantitative structure− activity relationship study of di-and tripeptides. *Journal of agricultural and food chemistry*, *54*(3), 732-738.

Figures

Fig. 1. Heat map of non-targeted UHPLC-QTOF-IMS profiles of LBPH fractions alcalase(AL),trypsin(TRY) & pepsin (PEP): (A) Amino Acids And Derivatives; (B) Sugars And Derivatives; (C) Lipids And Derivatives; (D) Vitamins And Terpinoids & Its Derivatives. (E) Flavonoids, Phenolic Acid And Its Derivatives

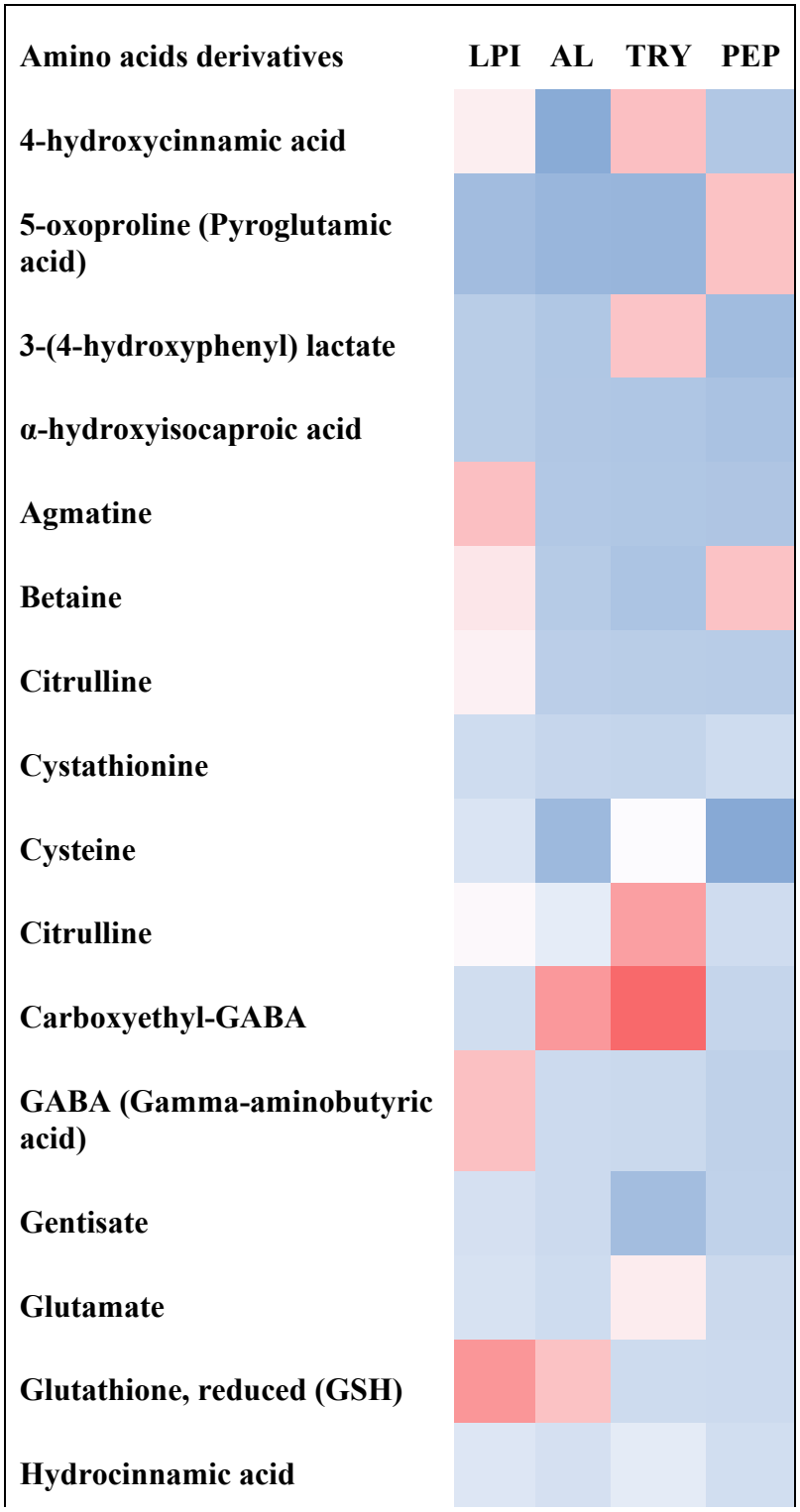

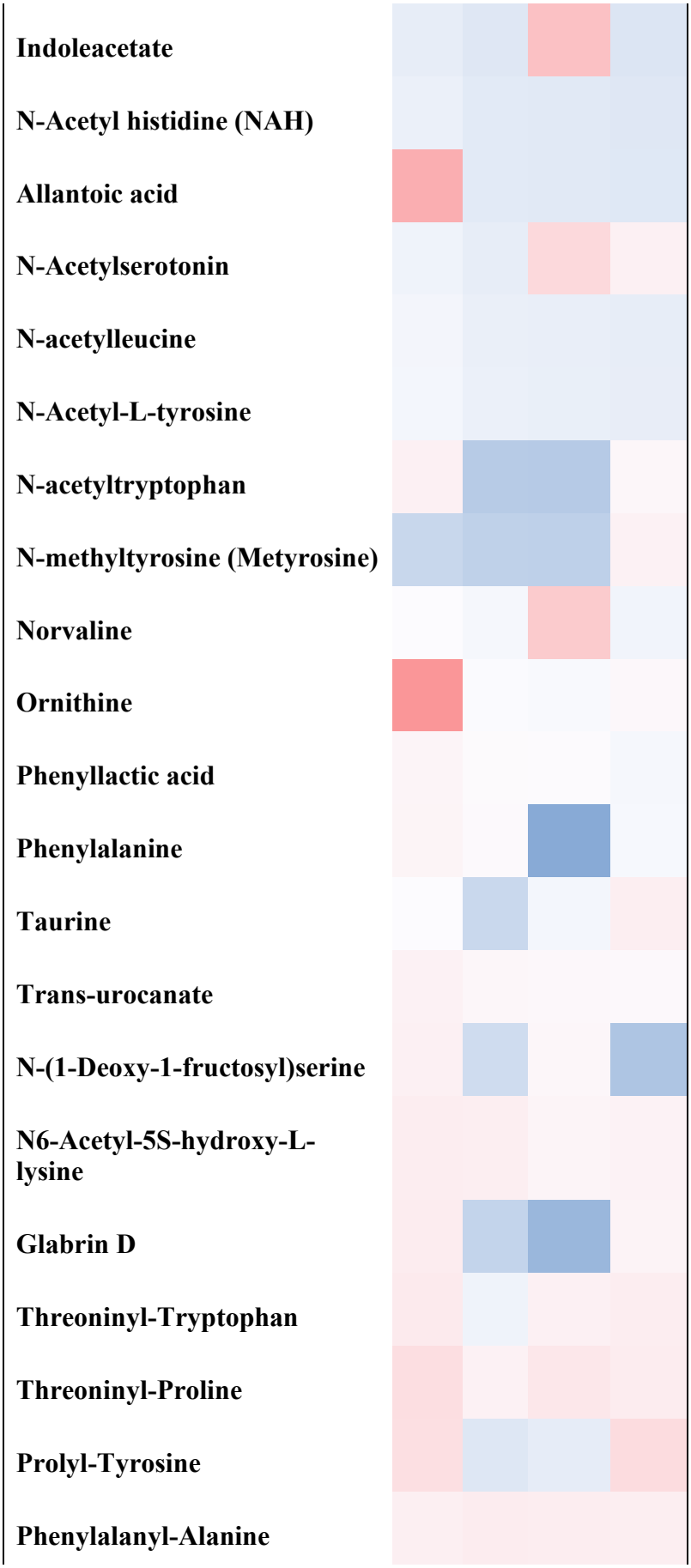
Indoleacetate
N-Acetyl histidine (NAH)
Allantoic acid
N-Acetylserotonin
N-acetylleucine
N-Acetyl-L-tyrosine
N-acetyltryptophan
N-methyltyrosine (Metyrosine)
Norvaline
Ornithine
Phenyllactic acid
Phenylalanine
Taurine
Trans-urocanate
N-(1-Deoxy-1-fructosyl)serine
N6-Acetyl-5S-hydroxy-L-lysine
Glabrin D
Threoninyl-Tryptophan
Threoninyl-Proline
Prolyl-Tyrosine
Phenylalanyl-Alanine

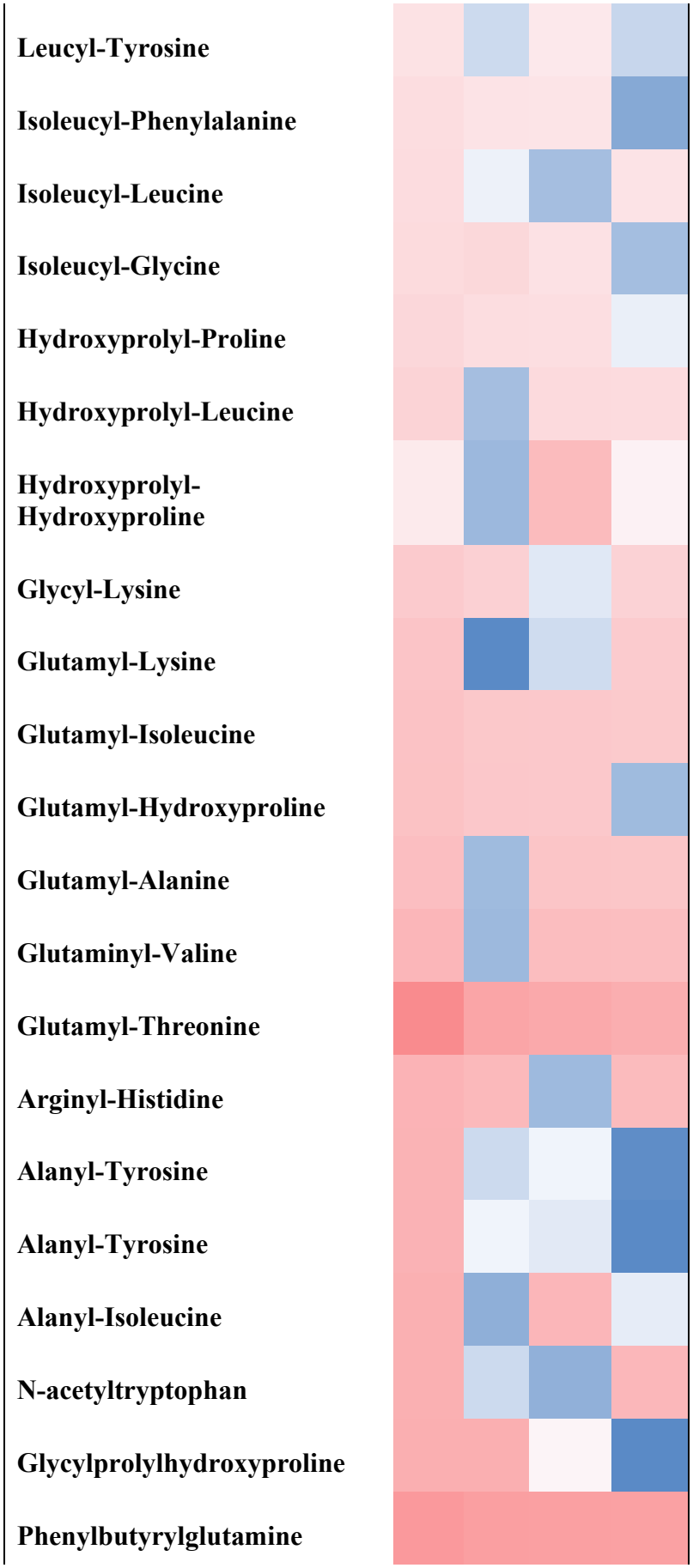
Leucyl-Tyrosine
Isoleucyl-Phenylalanine
Isoleucyl-Leucine
Isoleucyl-Glycine
Hydroxyprolyl-Proline
Hydroxyprolyl-Leucine
Hydroxyprolyl-
Hydroxyproline
Glycyl-Lysine
Glutamyl-Lysine
Glutamyl-Isoleucine
Glutamyl-Hydroxyproline
Glutamyl-Alanine
Glutaminyl-Valine
Glutamyl-Threonine
Arginyl-Histidine
Alanyl-Tyrosine
Alanyl-Tyrosine
Alanyl-Isoleucine
N-acetyltryptophan
Glycylprolylhydroxyproline
Phenylbutyrylglutamine

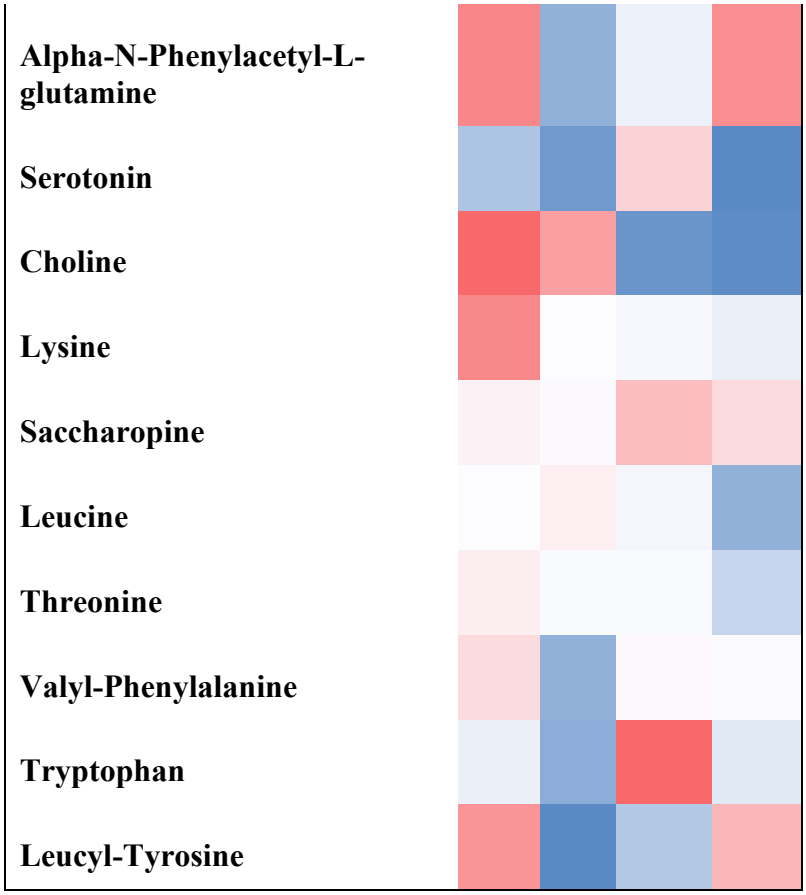
Alpha-N-Phenylacetyl-L-glutamine
Serotonin
Choline
Lysine
Saccharopine
Leucine
Threonine
Valyl-Phenylalanine
Tryptophan
Leucyl-Tyrosine

(A)

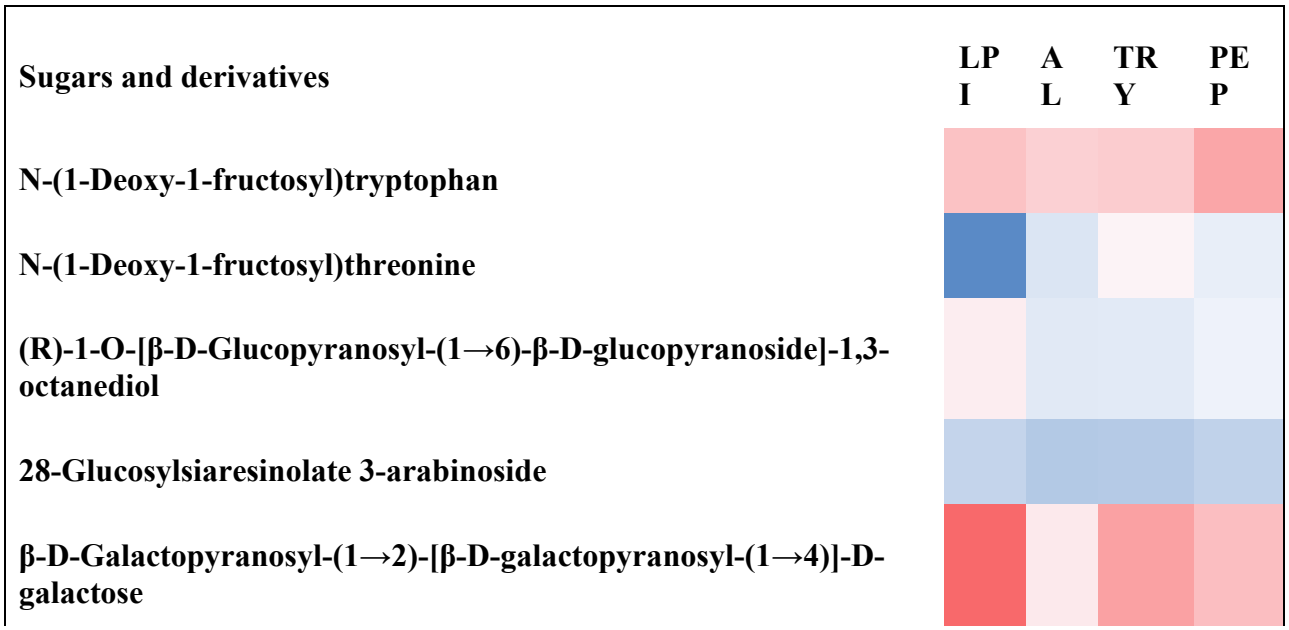
Sugars and derivatives
LPI
AL
TRY
PEP
N-(1-Deoxy-1-fructosyl)tryptophan
N-(1-Deoxy-1-fructosyl)threonine
(R)-1-O-[β-D-Glucopyranosyl-(1→6)-β-D-glucopyranoside]-1,3-octanediol
28-Glucosylsiaresinolate 3-arabinoside
β-D-Galactopyranosyl-(1→2)-[β-D-galactopyranosyl-(1→4)]-D-galactose

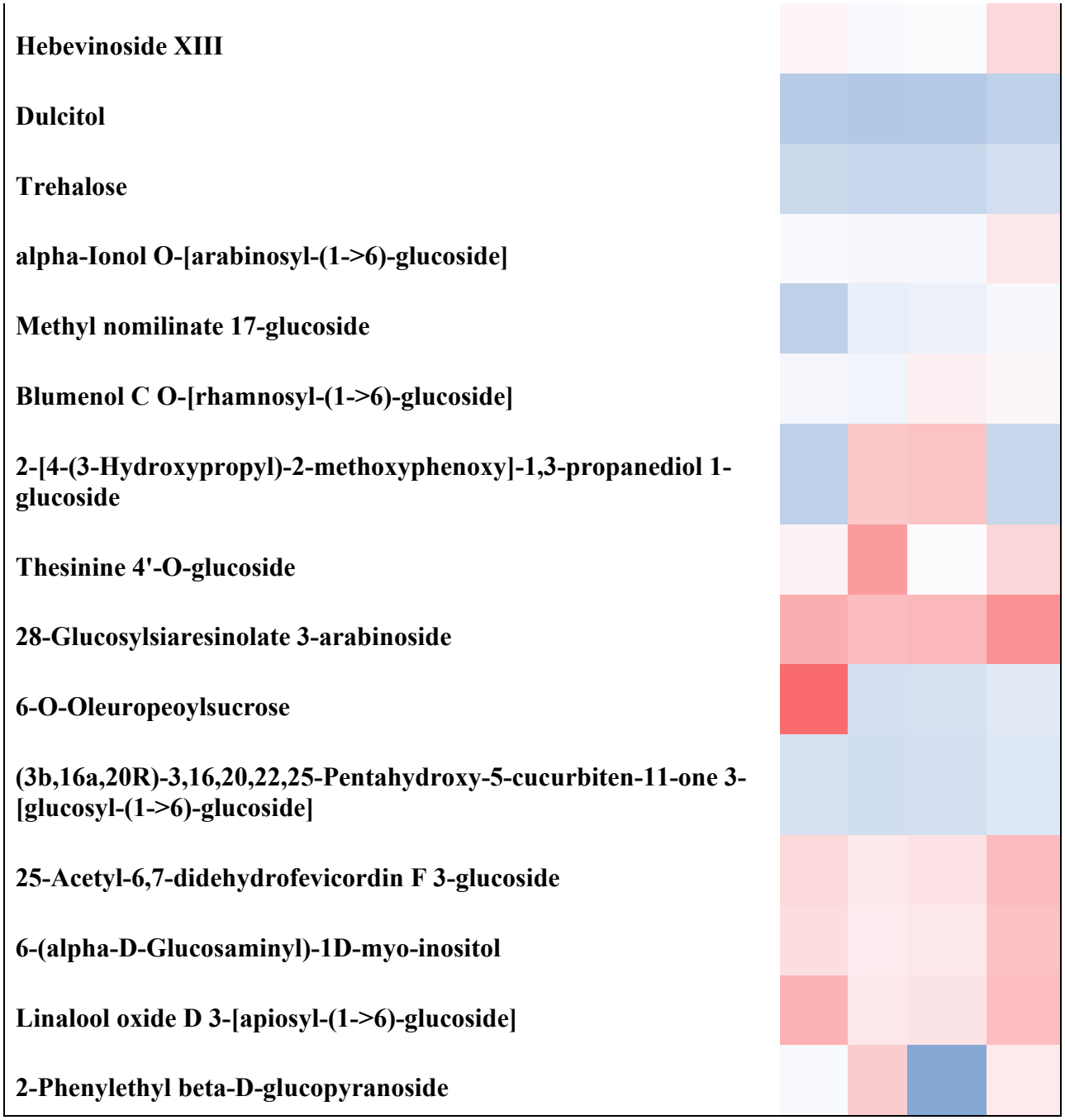

(B)

Lipids and its derivatives	LPI	AL	TRY	PEP

6-(alpha-D-Glucosaminyl)-1D-myo-inositol	
MG(16:1(9Z)/0:0/0:0)	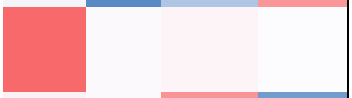
MG(0:0/16:0/0:0)	
LysoPE(0:0/20:1(11Z))	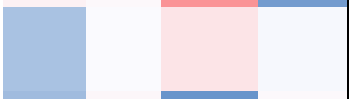
PG(18:0/22:5(7Z,10Z,13Z,16Z,19Z))	
CDP-DG(18:0/22:6(4Z,7Z,10Z,13Z,16Z,19Z))	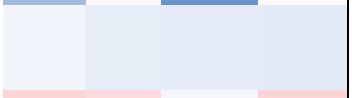
16-hydroxy hexadecanoic acid	
12-Oxo-Dodecenoic Acid	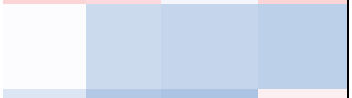
LysoPC 16:0	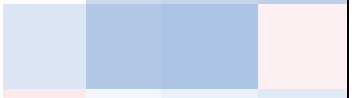
Hydroxy linolenic acid	
LysoPC 15:1	
Linolenic acid	
Linolenoyl glycerol	
2-Hydroxy palmitic acid	
Linoleoyl glycerol	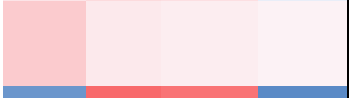
Linoleic acid	
Oleoyl glycerol	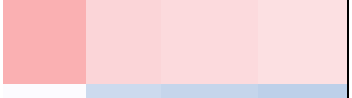
Ricinoleic acid	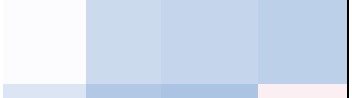
Eicosapentanoic acid	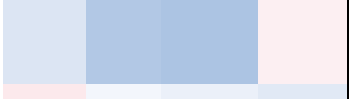
Oleic acid	
Methyl linolenic acid	

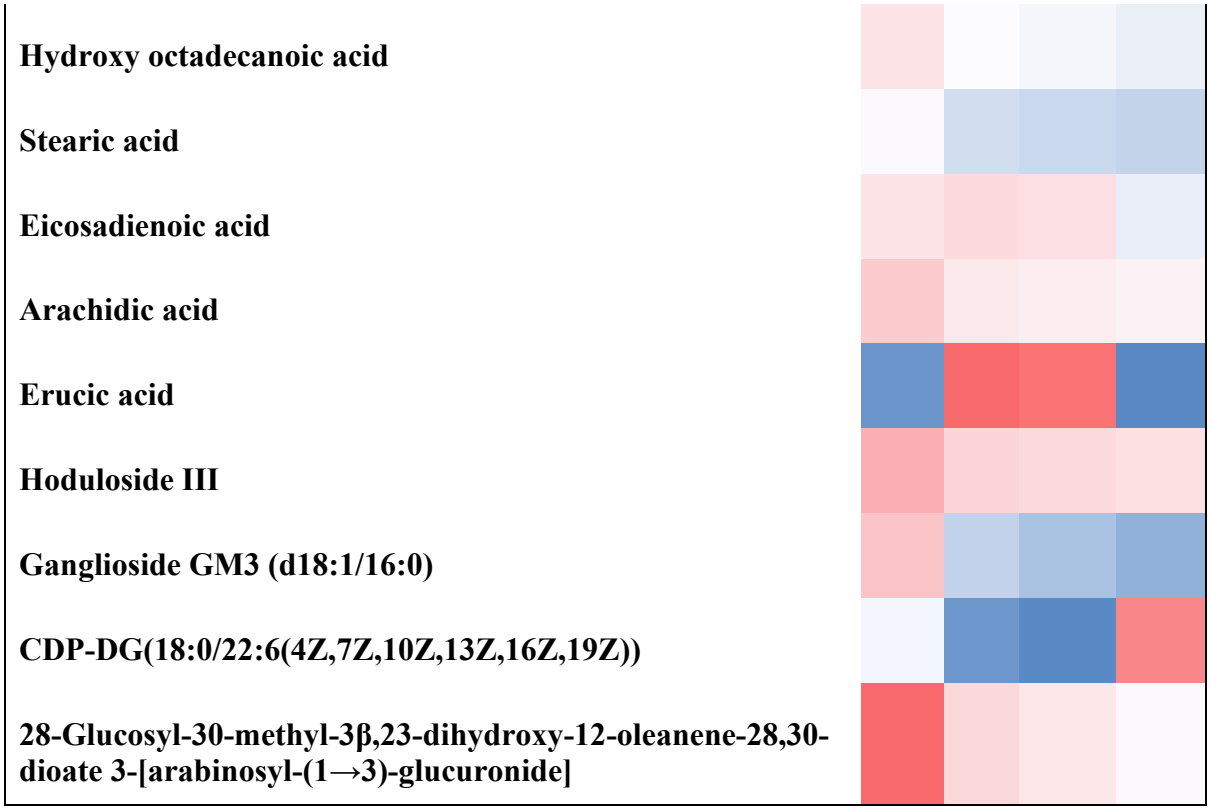
Hydroxy octadecanoic acid
Stearic acid
Eicosadienoic acid
Arachidic acid
Erucic acid
Hoduloside III
Ganglioside GM3 (d18:1/16:0)
CDP-DG(18:0/22:6(4Z,7Z,10Z,13Z,16Z,19Z))
28-Glucosyl-30-methyl-3β,23-dihydroxy-12-oleanene-28,30-dioate 3-[arabinosyl-(1→3)-glucuronide]

(C)

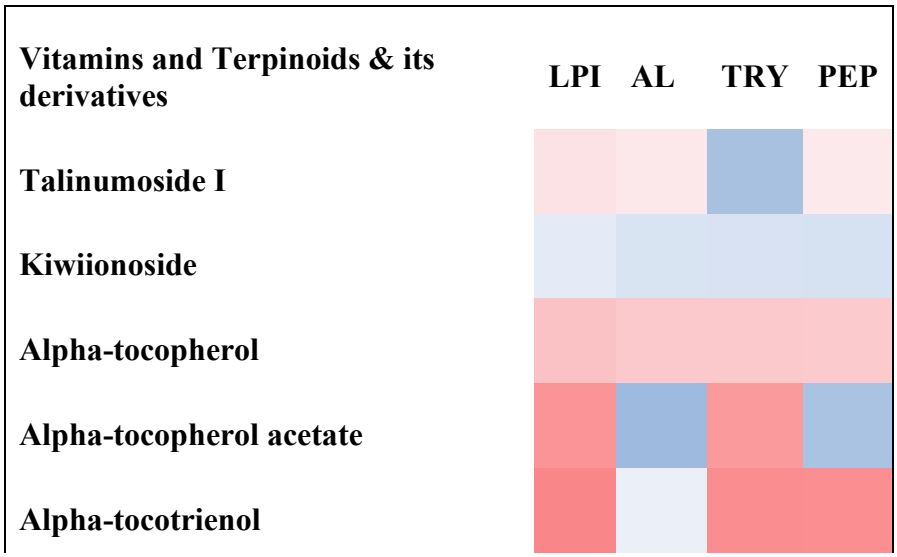
Vitamins and Terpinoids & its derivatives
LPI
AL
TRY
PEP
Talinumoside I
Kiwiionoside
Alpha-tocopherol
Alpha-tocopherol acetate
Alpha-tocotrienol

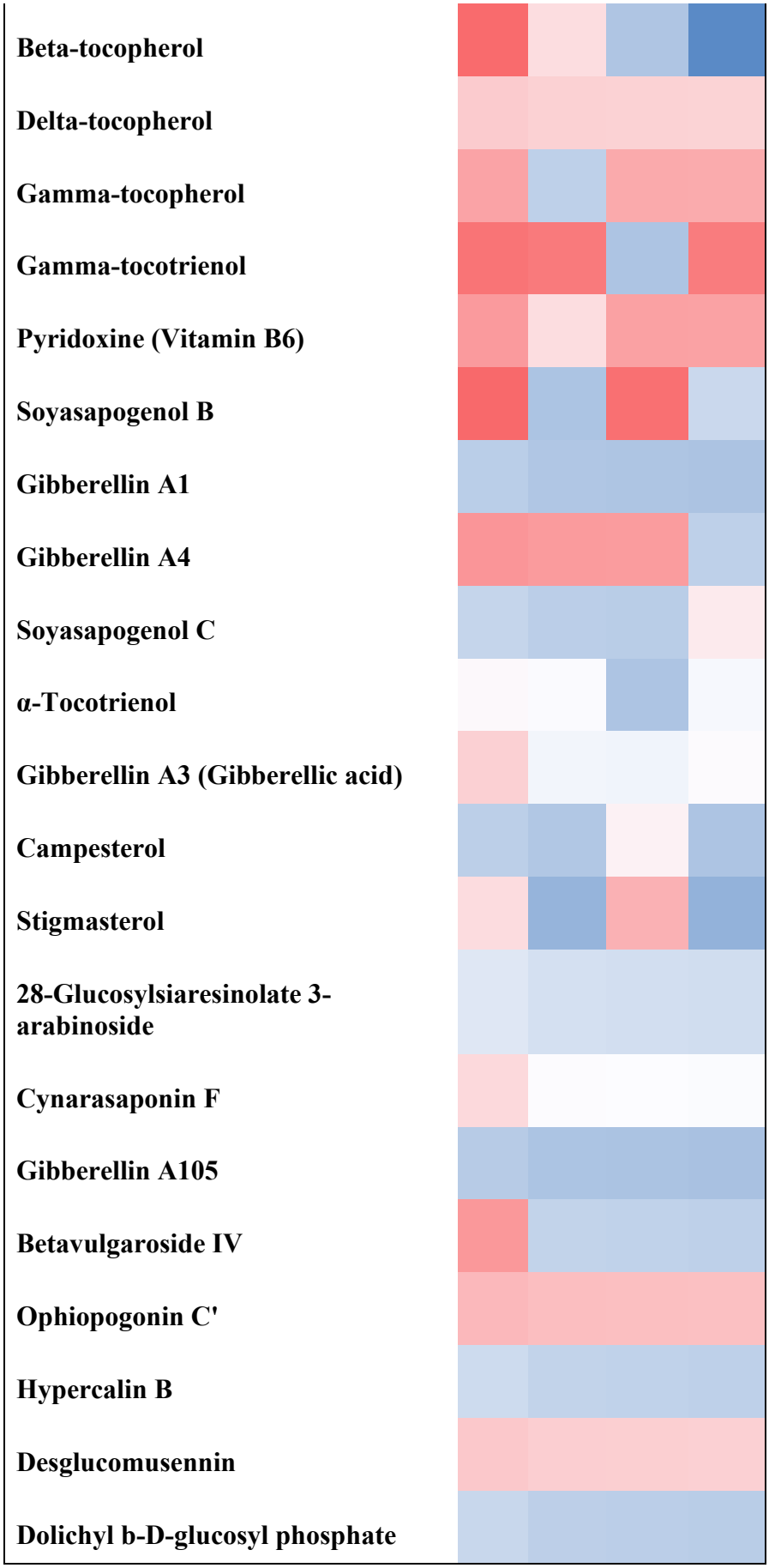
Beta-tocopherol
Delta-tocopherol
Gamma-tocopherol
Gamma-tocotrienol
Pyridoxine (Vitamin B6)
Soyasapogenol B
Gibberellin A1
Gibberellin A4
Soyasapogenol C
α-Tocotrienol
Gibberellin A3 (Gibberellic acid)
Campesterol
Stigmasterol
28-Glucosylsiaresinolate 3-arabinoside
Cynarasaponin F
Gibberellin A105
Betavulgaroside IV
Ophiopogonin C'
Hypercalin B
Desglucomusennin
Dolichyl b-D-glucosyl phosphate

(D)

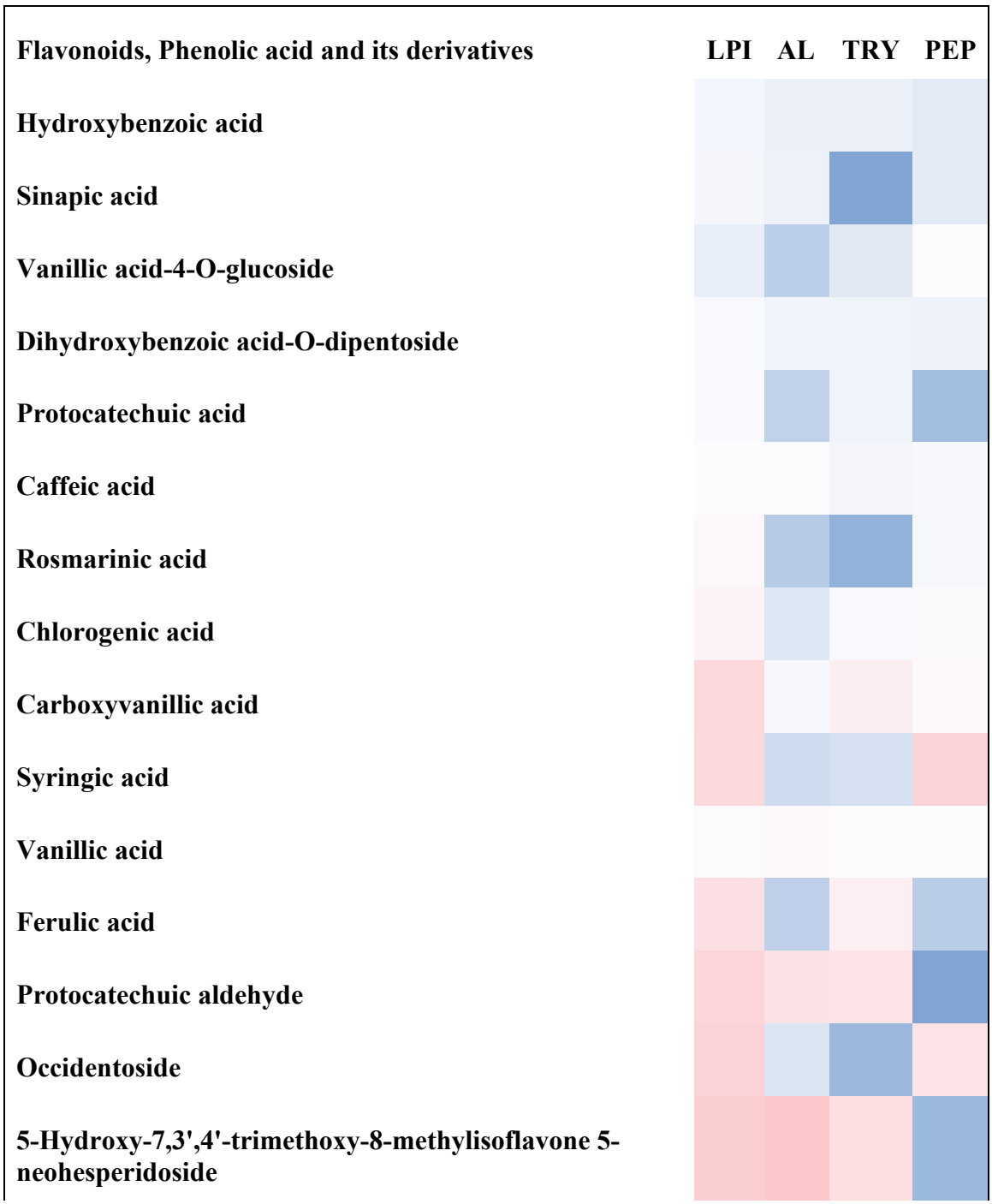
Flavonoids, Phenolic acid and its derivatives
LPI
AL
TRY
PEP
Hydroxybenzoic acid
Sinapic acid
Vanillic acid-4-O-glucoside
Dihydroxybenzoic acid-O-dipentoside
Protocatechuic acid
Caffeic acid
Rosmarinic acid
Chlorogenic acid
Carboxyvanillic acid
Syringic acid
Vanillic acid
Ferulic acid
Protocatechuic aldehyde
Occidentoside
5-Hydroxy-7,3',4'-trimethoxy-8-methylisoflavone 5-neohesperidoside

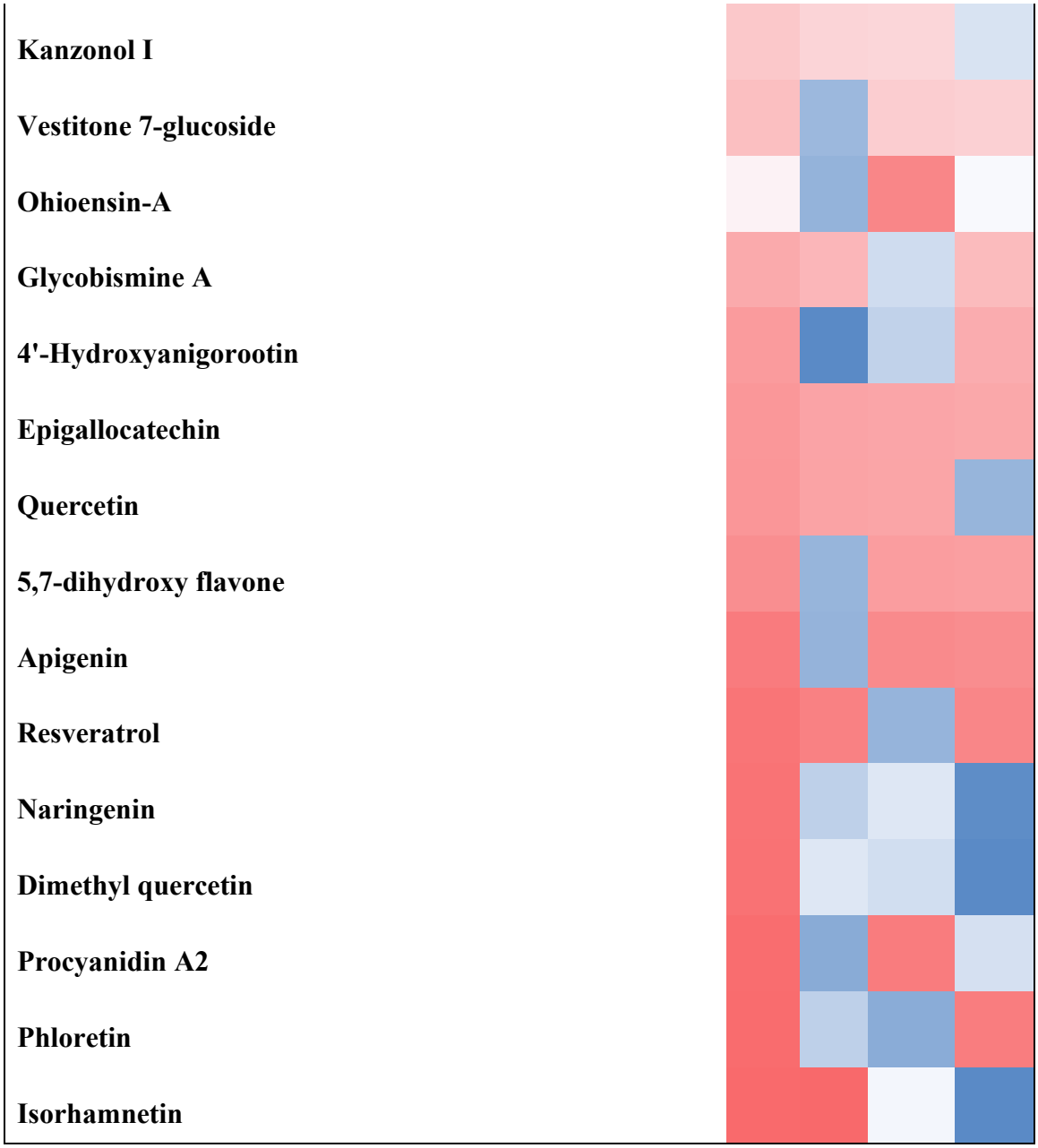

(E)

Heat map of non-targeted UHPLC-QTOF-IMS profiles of LBPH fractions (AL, PEP, TRY): (A) Amino Acids And Derivatives; (B) Sugars And Derivatives; (C) Lipids And Derivatives; (D) Vitamins And Terpinoids & Its Derivatives. (E) Flavonoids, Phenolic Acid And Its Derivatives

Figure 2(a): MALDI-TOF mass spectrum of the Alcalase-hydrolysed protein hydrolysates showing the distribution of detected ions according to their mass-to-charge ratio (m/z) and relative intensity.

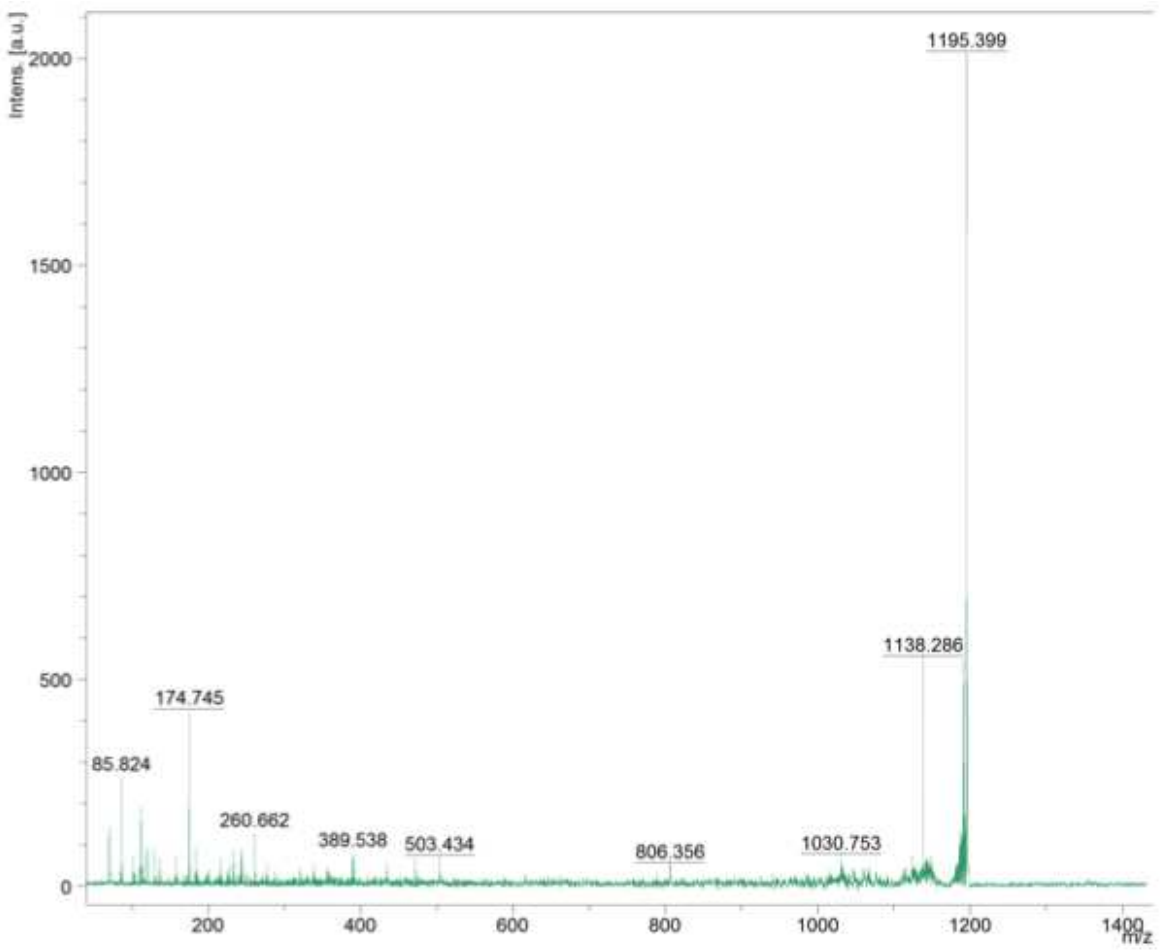

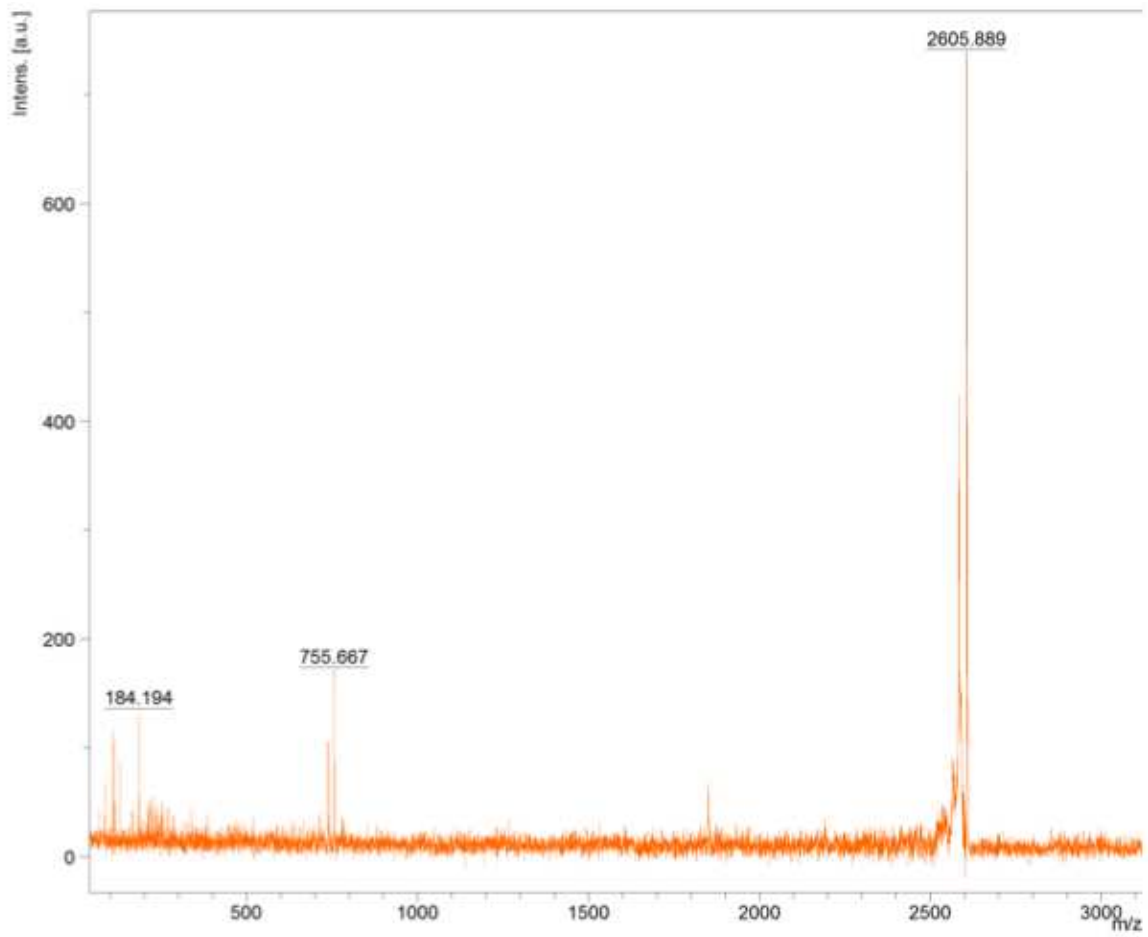

Figure 2(b): MALDI-TOF mass spectrum of the trypsin-hydrolysed protein hydrolysate showing the distribution of detected ions according to their mass-to-charge ratio (m/z) and relative intensity.

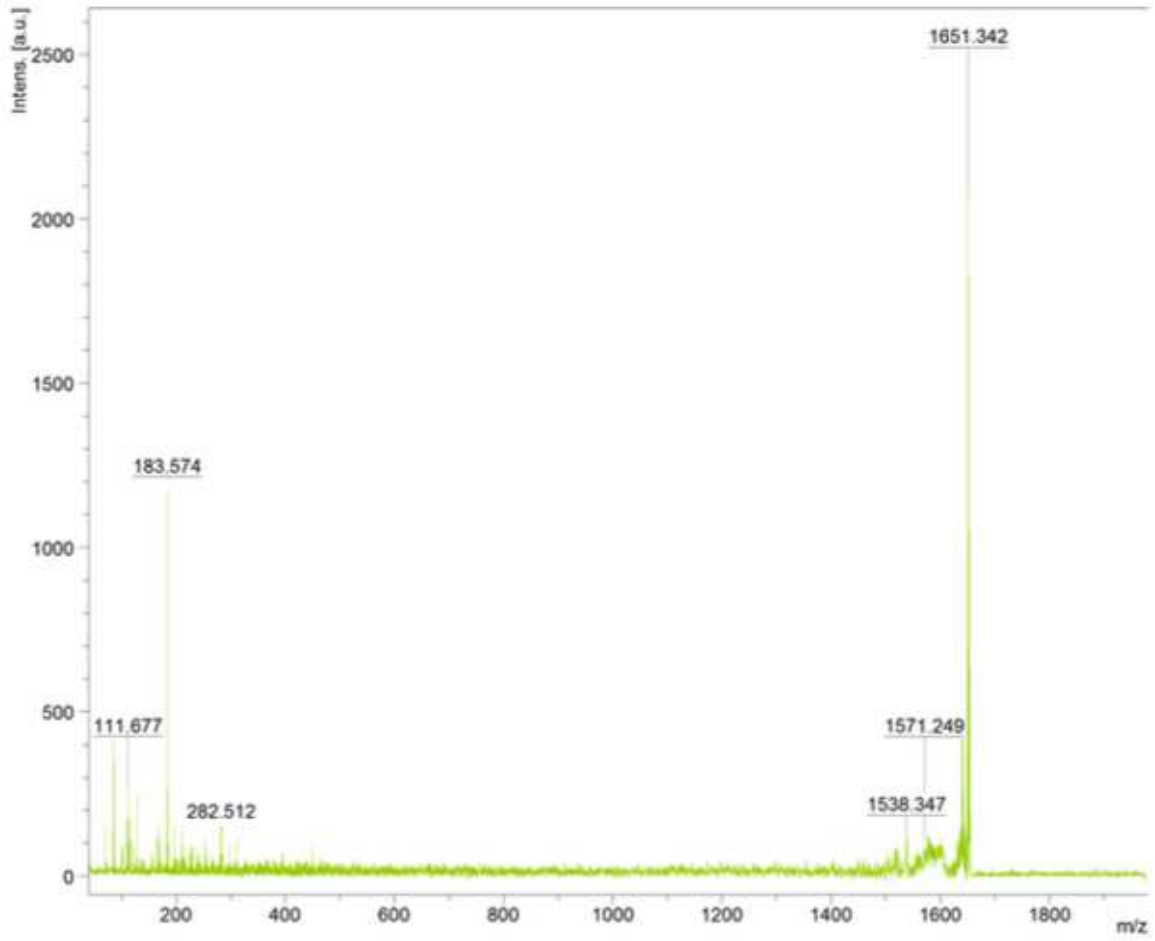

Figure 2(c): MALDI-TOF mass spectrum of the pepsin-hydrolysed protein hydrolysates showing the distribution of detected ions according to their mass-to-charge ratio (m/z) and relative intensity.

Fig 3(a). Molecular Docking of the Alcalase-Derived Lentil Peptide RLPALISRHQRL with Human Angiotensin-Converting Enzyme (ACE)

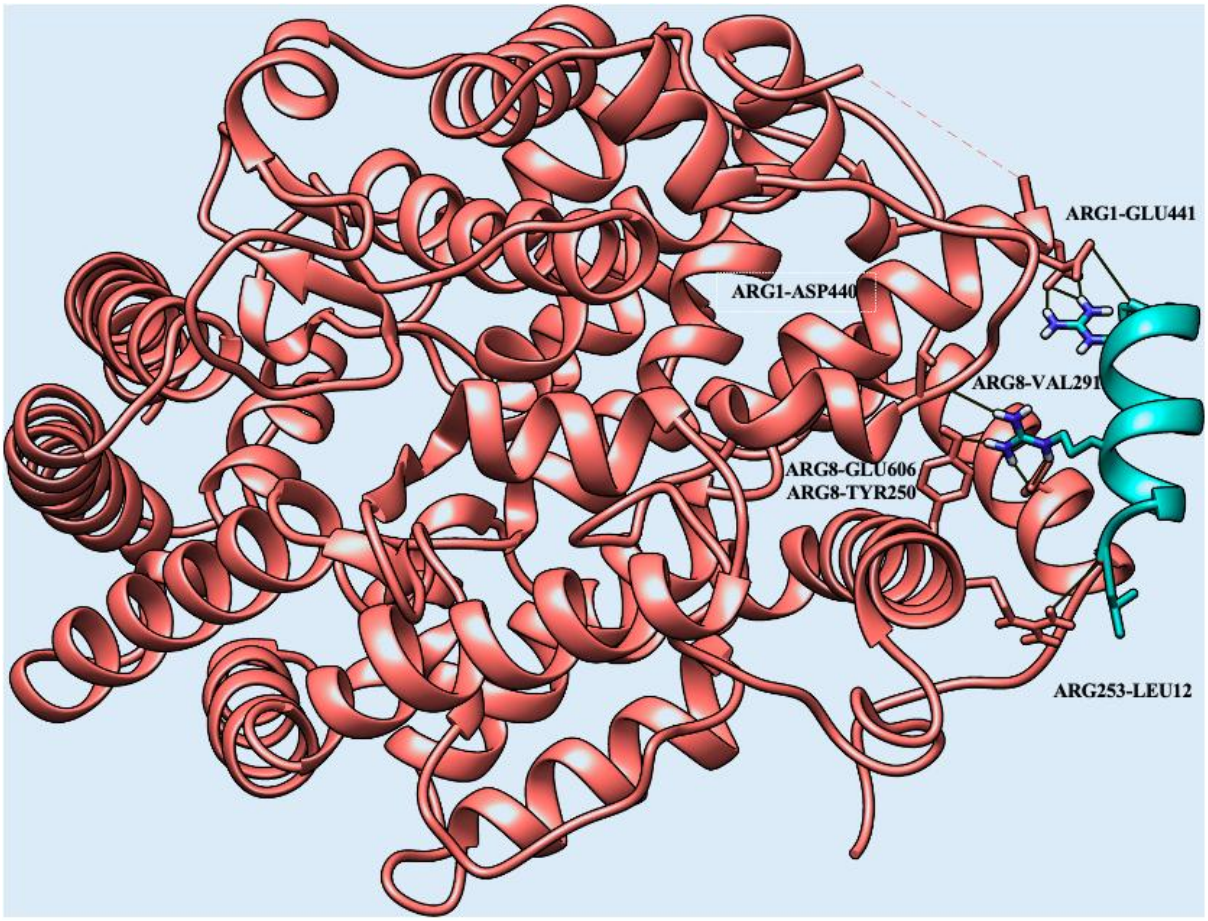

Molecular docking representation of the Alcalase-derived lentil peptide RLPALISRHQRL interacting with human angiotensin-converting enzyme (ACE; PDB ID: 1O8A). The ACE structure is depicted as a salmon-coloured ribbon, while the docked peptide is shown in cyan. The labelled residues indicate predicted contacts between the peptide and ACE, suggesting potential contributions from electrostatic interactions, hydrogen bonding, and hydrophobic contacts to complex stabilization.

Fig 3(b). Molecular Docking of the Trypsin-Derived Lentil Peptide RQPAAGEDSSEDLEDNTELLSLVLRA with Human Angiotensin-Converting Enzyme (ACE)

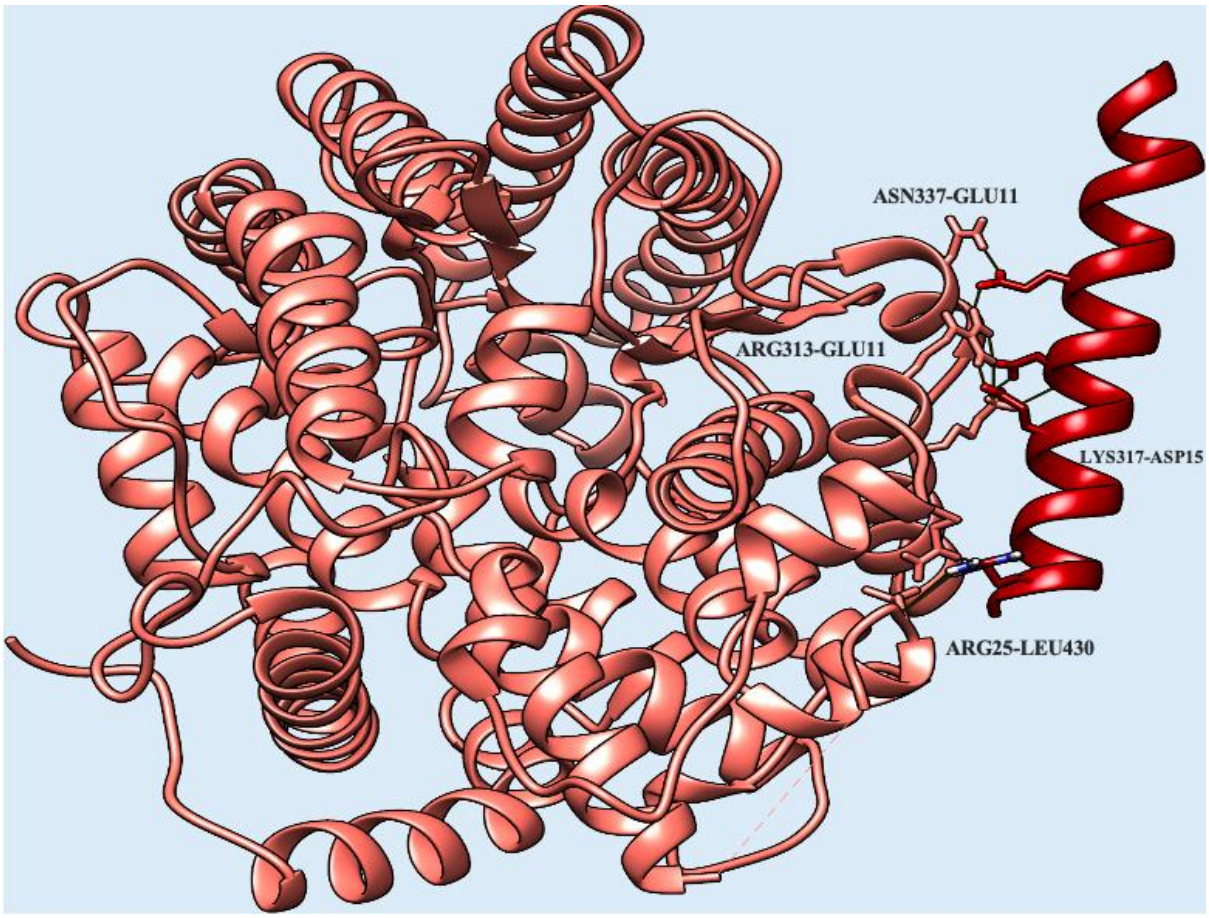

Molecular docking representation of the trypsin-derived lentil peptide

RQPAAGEDSSEDLEDNTELLSLVLRA interacting with human angiotensin-converting enzyme (ACE; PDB ID: 1O8A). ACE is represented as a salmon-coloured ribbon, while the docked peptide is shown in cyan. The labelled residue pairs, including Asn337–Glu11, Arg313–Glu11, Lys317–Asp15 and Arg25–Leu430, indicate predicted contacts between the peptide and ACE. These interactions suggest that polar and electrostatic contributions, together with local structural complementarity, may facilitate complex stabilization.

Fig 3(c). Molecular Docking of the Pepsin-Derived Lentil Peptide RLPAGVFFLGNFIGKGD with in the active site of human ACE (PDB: 1O8A).

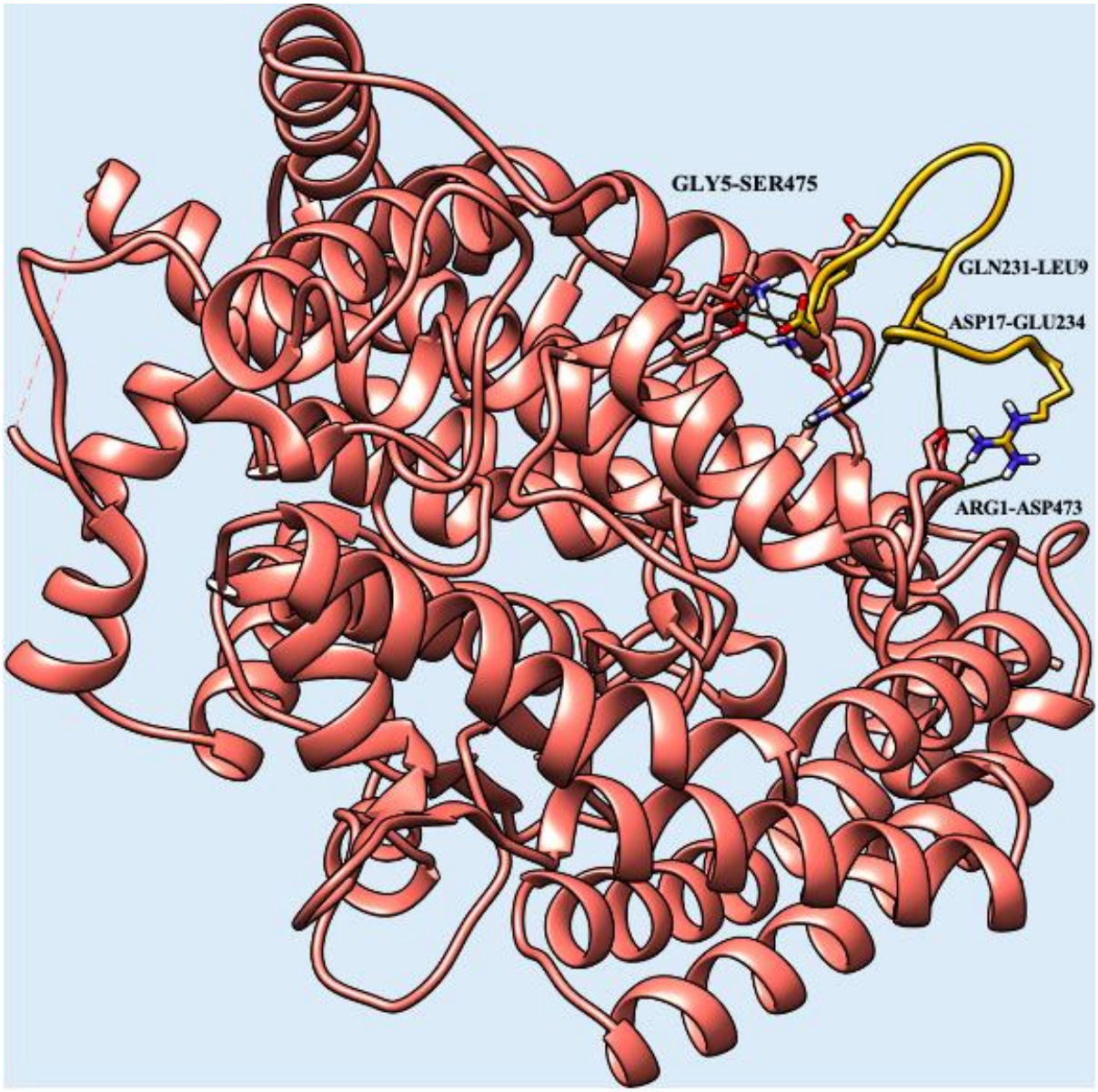

Molecular docking representation of the pepsin-derived lentil peptide RLPAGVFFLGNFIGKGD interacting with human angiotensin-converting enzyme (ACE; PDB ID: 1O8A). ACE is depicted as a salmon-coloured ribbon, while the docked peptide is represented in a contrasting stick representation. The labelled residue pairs, including Gln231–Leu9, Glu234–Asp17 and Asp473–Arg1, indicate predicted contacts within the docked complex. The peptide's hydrophobic and aromatic residues may contribute to interactions with non-polar regions of the ACE binding environment, while polar or charged residues may participate in additional stabilizing contacts.

Supplementary Files

This is a list of supplementary files associated with this preprint. Click to download.

- Tables.docx